

## Theoretical Study of the Kinetics of the Hydrogen Abstraction from Methanol. 2. Reaction of Methanol with Chlorine and Bromine Atoms

Jerzy T. Jodkowski,<sup>†</sup> Marie-Thérèse Rayez,\* and Jean-Claude Rayez

Laboratoire de Physicochimie Moléculaire, CNRS UMR 5803, Université Bordeaux I, 351, Cours de la Libération, 33405 Talence Cedex, France

Tibor Bérces and Sándor Dóbe

Central Research Institute for Chemistry, Hungarian Academy of Sciences, H-1525 Budapest, Hungary

Received: January 22, 1998; In Final Form: June 23, 1998

Ab initio calculations at different levels of theory and using several basis sets have been performed for the title two-channel hydrogen-abstraction reactions  $\text{CH}_3\text{OH} + \text{Cl}$  and  $\text{Br}$ . These calculations have shown that, similar to  $\text{CH}_3\text{OH} + \text{F}$ , both reactions proceed via formation of intermediate complexes. Rate constant calculations for this type of reactions have been performed using the equations developed in Jodkowski, J. T.; Rayez, M.-T.; Rayez, J.-C.; Bérces, T.; Sandor, D. *J. Phys. Chem.* **1998**, *102*, xxx. The very low energy barrier for the hydroxymethyl channel of the  $\text{CH}_3\text{OH} + \text{Cl}$  reaction obtained at the G2 level explains the relatively high value of the rate constant for this almost thermoneutral reaction. The very weak negative temperature dependence of the rate constant leading to  $\text{CH}_2\text{OH} + \text{HCl}$  observed experimentally is also well reproduced by the calculations. For the  $\text{CH}_3\text{OH} + \text{Br}$  reaction, both channels are endothermic, which explains the low values of the rate constants. A good agreement is obtained with experimental results and the temperature dependence of the rate constants. A temperature fit of the rate constants allows us to express them in a convenient way for chemical modeling studies:  $k(\text{CH}_2\text{OH}) = 4.8 \times 10^{-12} (T/300)^{2.6} \exp(-2975/T) \text{ cm}^3 \text{ molecule}^{-1} \text{ s}^{-1}$  and  $k(\text{CH}_3\text{O}) = 2.7 \times 10^{-12} (T/300)^{1.9} \exp(-9825/T) \text{ cm}^3 \text{ molecule}^{-1} \text{ s}^{-1}$ . In chlorine and bromine reactions, the channel leading to  $\text{CH}_3\text{O}$  is inactive at least for temperatures below 1000 K. The calculated potential energy surfaces have also allowed the determination of the rate constants for the reverse reactions  $\text{CH}_2\text{OH} + \text{HCl}$  and  $\text{HBr}$  which agree well with available experiments.

### 1. Introduction

The kinetic modeling studies of the pyrolysis and oxidation of methanol have been of great interest for chemists in the last several years,<sup>1</sup> in as much as methanol could be considered as an alternative, more environmental friendly fuel or fuel additive to gasoline. The hydrogen abstraction from methanol by atoms and radicals yields as products either hydroxymethyl or methoxy radicals in competing reaction channels according to the nonequivalent hydrogens of the methyl or hydroxyl group of  $\text{CH}_3\text{OH}$ . The efficiency of the product formation is described by its branching ratio, which is defined as the ratio of the rate constant for a given reaction channel divided by the sum of the rate constants of all parallel reaction channels. The reactive species formed in competing reaction channels may interfere each other or initiate different subsequent reactions. Therefore, knowledge of the branching ratios and their temperature dependence is of major importance for the chemical modeling studies. Despite their practical and theoretical importance, the kinetics of the H-abstraction from methanol by halogen atoms is not very well-known. Especially the branching ratio values at higher temperatures are reported with relatively large uncertainties.

The reaction of methanol with chlorine atom has been studied experimentally using either indirect<sup>2</sup> or direct<sup>3</sup> methods. The

results of measurements of the branching ratios for the channels



show a significant dominance of the hydroxymethyl reaction channel R2. The branching ratio for this latter channel has been found experimentally close to unity, 0.95.<sup>3f</sup> This is in agreement with what could be expected by comparing the heat of reaction of each channel. The hydroxymethyl reaction channel R2 should be favored as it is indeed weakly exothermic with a reaction enthalpy of  $-6.2 \text{ kcal/mol}$  at room temperature, while the methoxy channel R1 is endothermic by  $1.9 \text{ kcal/mol}$ . Moreover, the presence of three equivalent hydrogens on the methyl group leads to three reaction possibilities for R2. It was also found experimentally that the possible competing reaction related to the abstraction of OH group of methanol is negligible in comparison to abstraction of the methyl group hydrogen. Values of the overall rate constant (R1 + R2) obtained using direct techniques<sup>3</sup> are all in the range  $(5.3-6.3) \times 10^{-11} \text{ cm}^3 \text{ molecule}^{-1} \text{ s}^{-1}$ . Recent measurements by Dóbe et al.<sup>3e</sup> using the fast flow technique with LMR and EPR detections led to the rate constant of  $6.1 \times 10^{-11} \text{ cm}^3 \text{ molecule}^{-1} \text{ s}^{-1}$  at room temperature. This value, compared with the rate constants for H-abstraction from methanol by other atoms and radicals, is about factor of 2 lower than the one related to the analogous reaction of  $\text{CH}_3$  with fluorine<sup>3f</sup> ( $1.1 \times 10^{-10} \text{ cm}^3 \text{ molecule}^{-1}$

\* To whom correspondence should be addressed.

<sup>†</sup> Permanent address: Department of Physical Chemistry, Wrocław University of Medicine, Pl. Nankiera 1, 50-140 Wrocław, Poland.

s<sup>-1</sup>). However, due to the strength of the HF bond, both reaction channels for CH<sub>3</sub>OH + F are highly exothermic. On the other hand, the nearly thermoneutral reaction CH<sub>3</sub>OH + Cl has a rate constant 1 order of magnitude greater than the one observed in the case of the considerably more exothermic ( $\Delta H_{r,298} = -22.3$  kcal/mol for the hydroxymethyl reaction channel) reaction of methanol with OH ( $k = 9.1 \times 10^{-13}$  cm<sup>3</sup> molecule<sup>-1</sup> s<sup>-1</sup> at 298 K).<sup>3f</sup> The high value of the overall rate constant for the CH<sub>3</sub>OH + Cl reaction suggests that only a small or negligible energy barrier should be expected at least for the dominant reaction channel.

Kinetics and mechanism of the reaction of methanol with bromine is not well-known. Both overall rate constants or the branching ratios for the competing reaction channels



were obtained with unsatisfactory precision using indirect methods. One of the first investigations of CH<sub>3</sub>OH + Br was carried out by Buckley and Whittle,<sup>4a</sup> and Amphett and Whittle<sup>4b</sup> using conventional static or low flow photolysis. The reaction order and the corresponding overall rate constant determined experimentally were found to depend either on the chemical composition or on the pressure of the system. This was explained by a change in the nature of the termination reaction involving bromine atoms (hetero- and homogeneous recombination with other radicals). The Arrhenius parameters obtained for the temperature range 349–408 K lead, by extrapolation to room temperature, to a low value of the rate constant of  $2.4 \times 10^{-17}$  cm<sup>3</sup> molecule<sup>-1</sup> s<sup>-1</sup> for the hydroxymethyl reaction channel R4. Some information on the kinetics of the CH<sub>3</sub>OH + Br can be obtained from the direct study of the reverse reaction CH<sub>2</sub>OH + HBr → CH<sub>3</sub>OH + Br. However, the estimated value of the corresponding rate constant via equilibrium constant is not certain due to discrepancies of the order of ±1 kcal/mol in the enthalpy of formation of the hydroxymethyl.

Very recently, Dóbbé et al.<sup>5</sup> studied the CH<sub>3</sub>OH + Br reaction using excimer laser photolysis coupled with Br-atom resonance fluorescence detection over the temperature range 439–713 K. Results of this investigation lead to values of the rate constant larger than the ones estimated previously. Extrapolation of the rate constant from derived Arrhenius parameters leads to a value of  $1.1 \times 10^{-16}$  cm<sup>3</sup> molecule<sup>-1</sup> s<sup>-1</sup> at room temperature for R4. The branching ratio for hydroxymethyl formation was found close to unity, and the efficiency of the methoxy reaction channel was negligible even at the highest temperature of that investigation. Relatively low values of the rate constant for methanol reaction with bromine suggests high energy barriers for both reaction channels. A comparison of the branching ratio values for H-abstraction from methanol shows significant differences when the electronegative free radical reactant changes from F, Cl, and Br. At relatively low temperatures, practically all bromine<sup>3f</sup> and almost all chlorine<sup>3f</sup> are consumed by the hydroxymethyl reaction channel (R2 and R4) while the methoxy radical yield is higher than 50% in the CH<sub>3</sub>OH + F reaction.<sup>3f</sup>

In part 1,<sup>6</sup> it has been shown that the hydrogen abstraction from methanol by fluorine atoms proceeds via a complex mechanism. A similar reaction mechanism is also expected for the reaction of methanol with halogens, such as chlorine and bromine, with formation, in the first step of loosely bound intermediate complexes preceding the respective transition states. In this study, the theoretical analysis of the mechanism and

kinetics of the reactions under investigation is presented. This analysis concerns the ab initio search of the bound complexes and transition states of each reaction, and their structural (geometries and vibrational frequencies) analysis. Results of ab initio calculations allow the evaluation of the site-specific reaction rate constant and the branching ratios using computational methods of reaction rate theory.

## 2. Molecular Structure Calculation

**2.1. Details of Calculation.** Ab initio calculation were performed using the GAUSSIAN 92 and 94 program packages.<sup>7</sup> Restricted Hartree–Fock (RHF) self-consistent field (SCF) wave functions were used for closed shell molecules (CH<sub>3</sub>OH, HCl, and HBr) and unrestricted Hartree–Fock (UHF) SCF wave functions for the other open-shell species.<sup>8</sup> The electron correlation energy was estimated by Møller–Plesset perturbation theory<sup>9</sup> at the second (MP2) and up to fourth orders including all single, double, triple, and quadruple excitations (MP4SDTQ) and using the ‘frozen core’ approximation (the inner shells are excluded from the correlation energy calculation).<sup>7,10</sup> All equilibrium and transition states structures were fully optimized using the analytical gradients at SCF and MP2 levels with the 6-31G\* and 6-311G\*\* basis sets. For open-shell structures the spin contamination has been taken into account in the calculation of the energies by a projection method included in the Gaussian program and are noted in results as PMP2 and PMP4. Energies were also improved by using G1 and G2 levels of theory.<sup>11</sup> This approach is a composite procedure in which the geometries optimized at the MP2/6-31G\* level are used as reference in additional total energy calculations at MP4/6-311G\*\*, MP4/6-311+G\*\*, MP4/6-311G(2df,p), MP2/6-311+G(3df,2p), and QCISD(T)/6-311G\*\* in order to improve the calculated total energy. Temperature corrections to relative energies are obtained by using the calculated vibrational frequencies scaled by 0.8929 to take into account their overestimation at the (U)-HF/6-31G\* level.

**2.2. Geometries and Vibrational Levels.** CH<sub>3</sub>OH + Cl Reaction. Calculated optimized geometries and vibrational frequencies obtained at the MP2/6-311G\*\* levels of theory are given in Tables 1a and 1b and shown in Figure 1. In Table 1S of the Supporting Information these properties are given at the MP2/6-31G\* level.

**Transition state CH<sub>3</sub>O···H···Cl (TS1).** This transition state corresponds to the abstraction of the hydrogen atom from the hydroxyl group of methanol. The structural parameters depend only slightly on the level of theory as well as on the basis set used. The length of the breaking O···H<sub>o</sub> bond is 20% longer than the O–H bond in methanol. The formed H<sub>o</sub>···Cl bond is also about 20% longer than in isolated HCl (1.46 and 1.44 Å with the 6-31G\* and 6-311G\*\* basis set). Attack of the Cl-atom is far from collinear, as the O–H<sub>o</sub>–Cl angle is about 160° in the TS1 structure. Except in the MP2/6-31G\* calculation, a C<sub>s</sub> symmetry of methanol is found for the TS1 structure. The vibrational frequency values are weakly sensitive to the level of theory used. On the contrary, the value of the imaginary frequency obtained at the MP2 level is lower with the 6-31G\* basis set (2579i cm<sup>-1</sup>) than using the 6-311G\*\* basis set (2379i cm<sup>-1</sup>).

**Molecular complex CH<sub>3</sub>O···HCl (MC1).** The optimized structural parameters of this molecular complex where the methoxy radical is far from the hydrogen chlorine are shown on Figure 1. The shortest distance between CH<sub>3</sub>O and HCl is the distance O–H<sub>o</sub>. This distance depends on the level of theory used. It changes from 2.12 Å (UHF/6-311G\*\*) to 1.95 Å (MP2/

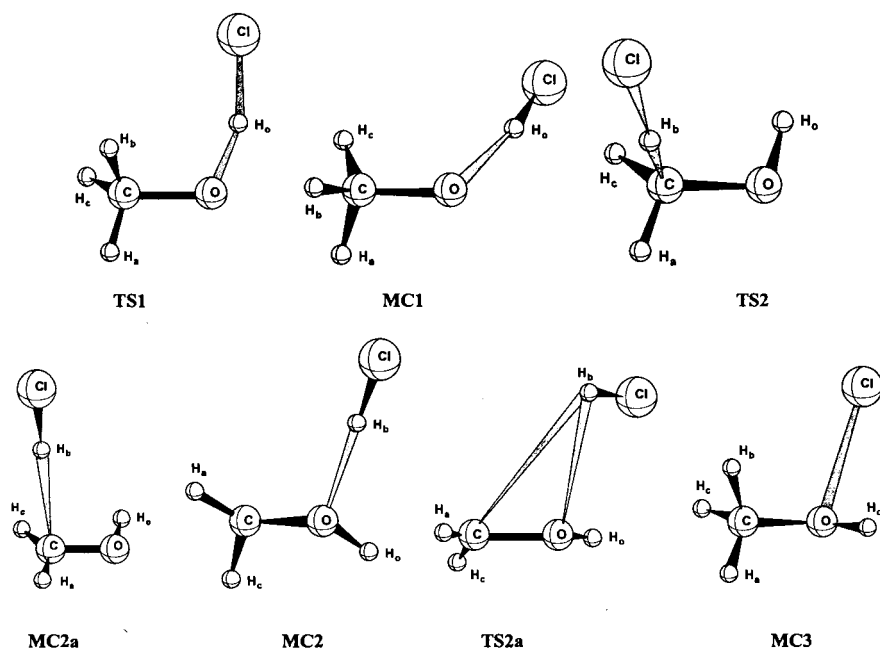


Figure 1. Geometrical structures of the intermediate structures and transition states found for the  $\text{CH}_3\text{OH} + \text{Cl}$  reaction.

TABLE 1: Optimized Structures of Stationary Points and Vibrational Frequencies of the Potential Energy Surface for the  $\text{CH}_3\text{OH} + \text{Cl}$  Reaction System Obtained at MP2/6-311G\*\* Level<sup>a</sup>

	TS1	MC1	TS2	MC2a	TS2a	MC2	MC3
(a) Vibrational Frequencies							
CO	1.3958	1.3816	1.3881	1.3595	1.3663	1.3748	1.4257
OH <sub>o</sub>	1.1829	1.9480	0.9598	0.9602	0.9601	0.9603	0.9603
CH <sub>a</sub>	1.0990	1.0944	1.0896	1.0816	1.0806	1.0799	1.0889
CH <sub>b</sub>	1.0935	1.1023	1.1556	2.1615	2.3900	2.8546	1.0947
CH <sub>c</sub>	1.0935	1.0952	1.0955	1.0862	1.0844	1.0838	1.0950
H <sub>o</sub> Cl	1.4435	1.2866					
H <sub>b</sub> Cl			1.7907	1.2896	1.2796	1.2865	
ClO							2.5417
COH <sub>o</sub>	112.2242	110.0499	107.5167	108.0962	108.0532	108.3660	107.0450
OCH <sub>a</sub>	103.8946	111.7716	108.8076	112.7860	112.8914	112.6026	106.5154
OCH <sub>b</sub>	112.2628	104.7156	111.3634	102.0031	77.5636	35.8986	111.9639
OCH <sub>c</sub>	112.2628	112.6651					
OH <sub>o</sub> Cl			114.6205	118.4964	118.5675	117.4521	
CH <sub>b</sub> Cl							111.2336
COCl	161.3798	168.7357	172.8238	172.9235	166.2090	154.5132	108.0029
H <sub>o</sub> OCH <sub>a</sub>	180.0000	-152.4453	173.4724	172.5488	171.4501	177.1085	177.5424
H <sub>o</sub> OCH <sub>b</sub>	63.0690	91.3791	-70.9845	-79.9302	-88.1932	-140.0875	58.8972
H <sub>o</sub> OCH <sub>c</sub>	-63.0690	-25.5179	48.1714	26.1430	23.2656	30.6573	-63.9958
ClH <sub>o</sub> OC	0.0000	1.9327					
ClH <sub>b</sub> CO			113.6368	71.8380	97.4682	178.9775	
ClOCH <sub>a</sub>							69.5753
(b) Optimized Structures							
$\nu_1$	172	55	64	37	61	54	98
$\nu_2$	196	83	166	107	108	88	133
$\nu_3$	516	157	440	129	172	150	172
$\nu_4$	660	424	1088	393	350	422	454
$\nu_5$	1030	500	1111	438	499	474	1076
$\nu_6$	1087	980	1147	538	757	550	1099
$\nu_7$	1201	1054	1309	830	1088	738	1196
$\nu_8$	1202	1130	1357	1096	1233	1090	1388
$\nu_9$	1435	1422	1428	1249	1395	1211	1510
$\nu_{10}$	1447	1437	1515	1401	1526	1388	1519
$\nu_{11}$	1540	1548	1954	1528	3001	1519	1532
$\nu_{12}$	3043	2898	3092	2828	3181	2908	3067
$\nu_{13}$	3131	3018	3205	3167	3330	3188	3144
$\nu_{14}$	3167	3108	3905	3316	3908	3340	3205
$\nu_{15}$	2379 <i>i</i>	3154	251 <i>i</i>	3907	154 <i>i</i>	3809	3899

<sup>a</sup> Bond lengths in angstroms, valence and dihedral angles in degrees,  $\nu_i$  in  $\text{cm}^{-1}$ .

6-311G\*\*). MC1 is significantly looser than the corresponding structure for  $\text{CH}_3\text{OH} + \text{F}$  reaction. The geometries of  $\text{CH}_3\text{O}$

and HCl are very close to those of the isolated species. The O-H<sub>o</sub>-Cl bond angle is close to 170°.

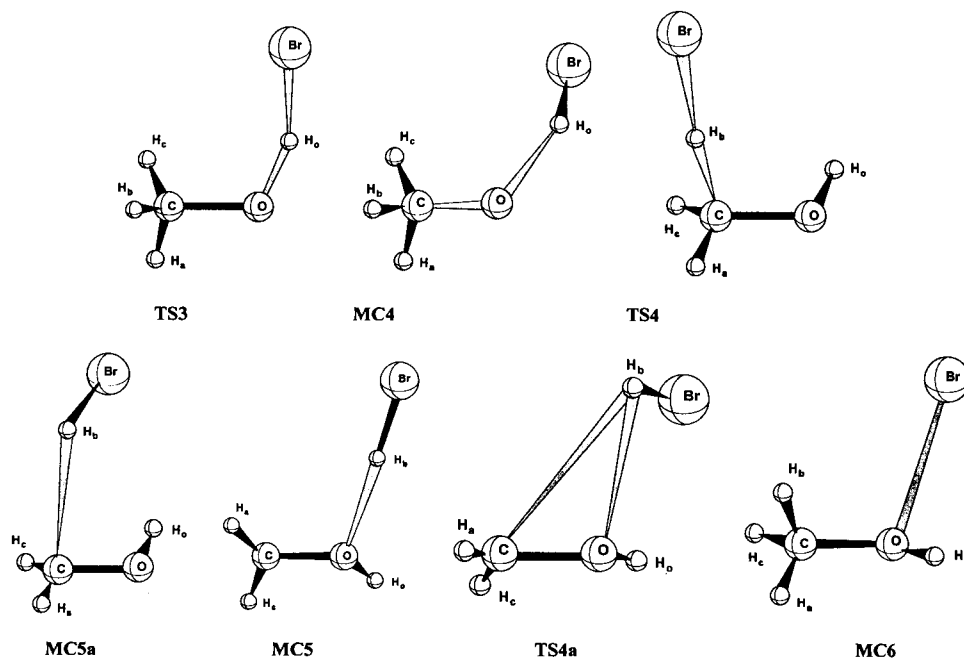


Figure 2. Geometrical structures of the intermediate and transition states found for the  $\text{CH}_3\text{OH} + \text{Br}$  reaction.

**Transition State  $\text{Cl}\cdots\text{H}\cdots\text{CH}_2\text{OH}$  (TS2).** The TS2 structure is more reactant-like than TS1, and attack of the chlorine atom is nearly collinear at any level of theory used. However, values of the other parameters depend significantly on the level of calculation as well as on the basis set used. The most sensitive structural parameters are the length of the breaking  $\text{C}\cdots\text{H}_b$  bond, which changes from 1.36 Å (UHF/6-31G\*) to 1.16 Å (MP2/6-311G\*\*) and the forming  $\text{H}_b\cdots\text{Cl}$  bond which goes from 1.52 to 1.79 Å, showing that the increase of the level of theory leads to a more reactant-like transition state. As a consequence of the larger  $\text{H}_b\text{—Cl}$  forming bond, the imaginary frequency has a very small value at the MP2/6-311G\*\* level of (251  $\text{cm}^{-1}$ ). The use of a mode-walking algorithm<sup>13</sup> confirms that this loose structure is a genuine transition state.

**Molecular Complexes  $\text{ClH}\cdots\text{CH}_2\text{OH}$ .**  $\text{ClH}\cdots\text{CH}_2\text{OH}$  denoted by MC2 and MC2a have been found as intermediates for the hydroxymethyl reaction channel. Both molecular complexes, which correspond to  $\text{H—Cl}$  at large distances from the hydroxyl radical, are very loose and formed due to hydrogen bonding. The optimized structure of MC2a (Table 1) is similar to the transition state TS2 with an almost collinear angle,  $\text{CH}_2\text{—Cl}$ , but the distance  $\text{C}\cdots\text{H}_b$  is somewhat larger (2.2 Å at MP2 level) and the  $\text{H}_b\text{—Cl}$  distance is almost the same as in the  $\text{H—Cl}$  molecule. This complex is slightly less stable than the molecular complex of hydroxymethyl with hydrogen chloride, MC2, which is, in fact, the most stable structure in the  $\text{CH}_3\text{OH} + \text{Cl}$  reaction system. In Figure 1, it is shown that this complex is stabilized by a weak hydrogen bond,  $\text{O}\cdots\text{H}_b$ . The  $\text{OH}_b\text{Cl}$  bond angle is nearly  $180^\circ$  and the structural parameters of the  $\text{CH}_2\text{OH}$  part of MC2 are very close to those obtained for the isolated hydroxymethyl radical.

**Transition state TS2a.** TS2a is a transition state for the isomerization  $\text{MC2a} \rightarrow \text{MC2}$  where the hydrogen chlorine part of MC2a is shifted in the direction of the oxygen of the hydroxymethyl. It leads to an elongation of the  $\text{C}\cdots\text{H}_b$  distance and a disappearance of the linearity of the  $\text{C}\cdots\text{H}_b\text{—Cl}$  atom system. Small values of the imaginary frequency of 30i (SCF) and 150–170i (MP2) show that the energy barrier for the  $\text{MC2a} \rightarrow \text{MC2}$  isomerization is broad.

**Molecular Complex MC3.** This molecular complex has a structure similar to the one found for the  $\text{CH}_3\text{OH} + \text{F}$  reaction system. MC3 is a very loose molecular complex. The distances between Cl and  $\text{CH}_3\text{OH}$  are long ( $\text{Cl}\cdots\text{O} = 2.5$  Å, and  $\text{Cl}\cdots\text{H}$  is longer than 3 Å at MP2 level). Other structural parameters have the same values as in the isolated methanol molecule. The set of vibrational frequencies of MC3 is formed of two parts, one part where the frequencies are almost identical to their corresponding values in methanol, and the three additional frequencies which are due to the Cl interaction and are less than  $200 \text{ cm}^{-1}$ .

**$\text{CH}_3\text{OH} + \text{Br}$  Reaction.** The optimized structures and vibrational frequencies of the characteristic points of the potential energy surface for the  $\text{CH}_3\text{OH} + \text{Br}$  reaction are given in Tables 2a and 2b. Calculations with the 6-311G\*\* basis set had computational problems both for bound complexes and transition states. Preset SCF convergence in energy could not be achieved despite the use of all convergent procedures included in the Gaussian 94 package. Similar difficulties with SCF convergence in the 6-311G\*\* basis set were previously reported by Chen and Tschuikow-Roux<sup>14</sup> both for a molecular complex and the transition state in the analogous calculation for H-abstraction reaction from ethane by bromine atoms. Hence, the electron correlation corrections were carried out only with the 6-31G\* basis set, and G2MP2, G2MP3, G1, and G2 energies<sup>11</sup> are available only for reactants and products molecules.

**Transition State  $\text{CH}_3\text{O}\cdots\text{H}\cdots\text{Br}$  (TS3).** This transition state shown in Figure 2 and described in Table 2 describes the attack of a bromine atom on the hydrogen atom of the hydroxyl group of  $\text{CH}_3\text{OH}$ . In this structure, the bromine atom is about  $60^\circ$  out of the  $\text{COH}_b$  plane. The breaking  $\text{O—H}_b$  bond length found by MP2/6-31G\* calculations is 1.28 Å. This corresponds to a relative elongation of 30% with respect to the OH bond length in the methanol molecule. On the contrary, the forming  $\text{H}_b\cdots\text{Br}$  bond distance is found at 1.57 Å as having a reactant-like character. As in the case of TS1, the value of the imaginary frequency is around  $1900 \text{ cm}^{-1}$  in the MP2 calculation.

**Molecular Complex  $\text{CH}_3\text{O}\cdots\text{HBr}$  (MC4).** Structural parameters of the complex of methoxy radical with HBr are close



**TABLE 2: Optimized Structures of Stationary Points and Vibrational Frequencies of the Potential Energy Surface for the CH<sub>3</sub>OH + Br Reaction System Obtained at the MP2/6-31G\* Level<sup>a</sup>**

	TS3	MC4	TS4	MC5a	TS4a	MC5	MC6
(a) Optimized Structures							
CO	1.4039	1.3932	1.3596	1.3682	1.3760	1.3832	1.4354
OH <sub>o</sub>	1.2825	1.9795	0.9735	0.9736	0.9725	0.9724	0.9730
CH <sub>a</sub>	1.0998	1.0944	1.0847	1.0813	1.0809	1.0800	1.0886
CH <sub>b</sub>	1.0925	1.1013	1.5885	2.4672	3.0451	2.7798	1.0940
CH <sub>c</sub>	1.0934	1.0946	1.0900	1.0873	1.0853	1.0843	1.0947
H <sub>o</sub> Br	1.5690	1.4500					
H <sub>b</sub> Br			1.5445	1.4438	1.4376	1.4511	
BrO							2.6241
COH <sub>o</sub>	112.9450	102.9303	109.4006	108.5581	108.3771	108.9915	107.9219
OCH <sub>a</sub>	102.3192	111.1539	111.6155	112.2605	112.2917	112.0661	105.9142
OCH <sub>b</sub>	112.8591	104.5512	106.8149	88.8163	59.4887	39.8263	111.7193
OCH <sub>c</sub>	112.1817	112.3113	117.7597	118.1448	118.0758	117.3422	110.9302
OH <sub>o</sub> Br	142.5809	158.7805					
CH <sub>b</sub> Br			172.0199	124.8775	111.5777	149.2771	
COBr							106.2697
H <sub>o</sub> OCH <sub>a</sub>	161.0833	-147.9738	173.5334	178.9869	173.4116	178.3245	177.0090
H <sub>o</sub> OCH <sub>b</sub>	43.5123	95.7808	-76.0900	-47.2657	-70.0566	-127.6865	58.3948
H <sub>o</sub> OCH <sub>c</sub>	-83.3639	-21.6113	32.9116	34.4755	28.0865	33.3002	-64.5182
BrH <sub>o</sub> OC	59.2477	6.5317					
BrH <sub>b</sub> CO			54.7071	49.0949	88.2283	175.5978	
BrOCH <sub>a</sub>							73.9037
(b) Vibrational Frequencies							
$\nu_1$	160	79	65	86	59	40	108
$\nu_2$	187	97	236	106	108	86	131
$\nu_3$	302	160	538	137	135	137	170
$\nu_4$	725	372	760	260	247	392	455
$\nu_5$	1032	485	854	366	560	459	1063
$\nu_6$	1203	982	982	563	787	544	1096
$\nu_7$	1265	1078	1119	854	1104	779	1201
$\nu_8$	1305	1135	1254	1115	1224	1098	1399
$\nu_9$	1481	1457	1318	1240	1413	1202	1527
$\nu_{10}$	1488	1489	1413	1418	1545	1393	1561
$\nu_{11}$	1577	1573	1546	1548	2666	1538	1569
$\nu_{12}$	3070	2513	3167	2589	3207	2504	3101
$\nu_{13}$	3165	3051	3315	3191	3356	3218	3183
$\nu_{14}$	3209	3146	3763	3346	3774	3372	3245
$\nu_{15}$	1900 <i>i</i>	3192	331 <i>i</i>	3757	113 <i>i</i>	3781	3767

<sup>a</sup> Bond lengths in angstroms, valence and dihedral angles in degrees,  $\nu_i$  in cm<sup>-1</sup>.

to each other at both levels of theory used. Indeed only the O–H<sub>o</sub> bond distance depends on the type of calculation (2.0 Å at MP2). At both MP2 and SCF levels, the highest vibrational frequency corresponding to the O–H<sub>o</sub> stretch is significantly lowered (by 800 cm<sup>-1</sup> for SCF and 600 cm<sup>-1</sup> for MP2) in comparison to the O–H stretch in methanol.

**Transition State Br···H···CH<sub>2</sub>OH (TS4).** For this structure (Table 2), the attack of the bromine atom on the H atom of the methyl part of methanol is nearly collinear. Structural parameters depend only slightly on the level of calculation. The length of the breaking C–H<sub>b</sub> bond obtained at MP2 level is 1.59 Å, which corresponds to a relative elongation of the C–H bond of 45% compared to parent methanol. On the other hand, the formed H<sub>b</sub>···Br bond distance of 1.54 Å at MP2 level is only 10% larger than the bond length of isolated HBr molecule. These characteristics correspond to a product-like transition state.

**Molecular Complex BrH···CH<sub>2</sub>OH (MC5 and MC5a).** Similar to the analogous structures for the CH<sub>3</sub>OH + Cl reaction system, molecular complexes of hydroxymethyl with hydrogen bromine are in a fact formed by weak hydrogen bonding. The optimized geometry of MC5a significantly depends on the method used. The contact distance for C···H<sub>b</sub> of 2.5 Å found in MP2 calculation is almost 1.5 Å shorter than that obtained at the SCF level. The MP2 value of 124° for the C···H<sub>b</sub>···Br bond angle is very different from the almost collinear atom system C···H<sub>b</sub>···Cl in the corresponding molecular complex MC2a. The complex MC5 is also a loose structure, with

O···H<sub>b</sub> distances of ca. 2.8 Å at the MP2 level. Values of other structural parameters both bond lengths or valence and dihedral angles are close for both methods used. The vibrational frequencies larger than  $\nu_6$  are very close to their corresponding counterparts in hydroxymethyl.

**Transition State TS4a** is a saddle point for the isomerization MC5a → MC5. Its structure presented in Figure 2 shows some similarity to TS2a; however, H<sub>b</sub> atom is farther away from the C–O bond of hydroxymethyl. TS4a is very loose, with contact distances C···H<sub>b</sub> of 3.0–4.2 Å and O···H<sub>b</sub> of 2.6–3.0 Å depending on the method used. The imaginary frequency is close to that of TS2a (113*i* at MP2 level).

**Molecular complex MC6.** The structure of this complex is very close to analogous complexes which are formed by fluorine and chlorine with methanol. MC6 is the most stable structure for CH<sub>3</sub>OH + Br reaction system. Contact distances between bromine, oxygen, and hydrogen atoms of CH<sub>3</sub> and OH groups of methanol are greater than 3.0 Å. Geometrical parameters of both SCF and MP2 optimized structures are close. Vibrational frequencies obtained at SCF and MP2 levels are also close to each other, and (as for MC5) the conserved frequencies are almost identical to those of the methanol molecule.

**2.3. Energetics and Mechanism of the CH<sub>3</sub>OH + Cl and CH<sub>3</sub>OH + Br Reactions.** In Tables 3–4 are given the relative energies (including respective zero-point vibrational energy corrections) of characteristic points of the potential energy surface at different levels of theory with respect to the reactants

**TABLE 3: Relative Energies, with Respect to Reactant Energy, of Stationary Points of the Potential Energy Surface at 0 K for CH<sub>3</sub>OH + Cl Reaction System Calculated at Different Levels of Theory<sup>a</sup>**

molecular system		PMP2 <sup>b</sup>	MP4 <sup>c</sup>	G2MP2	G2MP3	G1	G2	exptl <sup>d</sup>
CH <sub>3</sub> OH + HCl		-5.7	-4.6	-7.2	-6.8	-5.3	-6.4	
		<b>-5.1</b>	<b>-4.0</b>	<b>-6.6</b>	<b>-6.2</b>	<b>-4.7</b>	<b>-5.8</b>	<b>-6.8 ± 1.0</b>
ClH...CH <sub>2</sub> OH	(MC2)	-10.1	-8.7	-10.9	-10.5	-9.5	-10.0	
TS2a		-8.2	-6.9					
MC2a		-7.9	-6.7					
Cl...H...CH <sub>2</sub> OH	(TS2)	-0.5	0.3	-5.6	-5.2	-4.5	-5.0	
MC3		-4.2	-2.7	-5.1	-5.0	-5.2	-5.1	
CH <sub>3</sub> O...H...Cl	(TS1)	11.3	11.0	7.7	7.9	8.0	8.1	
CH <sub>3</sub> O...HCl	(MC1)	1.4	-0.9	-1.8	-2.0	-0.7	-1.4	
CH <sub>3</sub> O + HCl		5.3	2.8	2.1	1.9	3.1	2.4	
		<b>5.7</b>	<b>3.2</b>	<b>2.5</b>	<b>2.3</b>	<b>3.5</b>	<b>2.8</b>	<b>2.3 ± 1.0</b>

<sup>a</sup> In kcal/mol; bold type (in product rows) shows the reaction enthalpy at 298 K. <sup>b</sup> PMP2/6-311G\*\*//MP2/6-311G\*\* energy with ZPE calculated using the unscaled MP2/6-311G\*\* frequencies. <sup>c</sup> MP4SDTQ/6-311G\*\*//MP2/6-311G\*\* energy with ZPE calculated using the unscaled MP2/6-311G\*\* frequencies. <sup>d</sup> Calculated using the enthalpies of formation from refs 5 and 15.

**TABLE 4: Relative Energies, with Respect to Reactant Energy, of Stationary Points of the Potential Energy Surface at 0 K for CH<sub>3</sub>OH + Br Reaction System Calculated at Different Levels of Theory<sup>a</sup>**

molecular system		PMP2 <sup>b</sup>		MP4 <sup>c</sup>		G2MP2	G2MP3	G1	G2	exptl <sup>d</sup>
CH <sub>3</sub> OH + HBr		9.9	(10.1)	10.3	(10.4)	6.4	6.5	6.8	6.7	
		<b>10.5</b>	<b>(10.6)</b>	<b>10.8</b>	<b>(11.0)</b>	<b>7.0</b>	<b>7.1</b>	<b>7.4</b>	<b>7.3</b>	<b>8.8 ± 1.0</b>
BrH...CH <sub>2</sub> OH	(MC5)	5.3	(5.1)	6.2	(6.0)					
TS4a		6.6	(5.5)	7.2	(6.1)					
MC5a		6.7	(6.3)	7.2	(6.8)					
Br...H...CH <sub>2</sub> OH	(TS4)	6.7	(6.5)	8.7	(8.5)					
MC6		-6.5	(-6.8)	-6.3	(-6.6)					
CH <sub>3</sub> O...H...Br	(TS3)	19.9	(19.0)	18.1	(17.3)					
CH <sub>3</sub> O...HBr	(MC4)	11.8	(11.6)	8.5	(8.3)					
CH <sub>3</sub> O + HBr		16.2	(16.4)	12.5	(12.7)	15.8	15.2	15.2	15.5	
		<b>16.6</b>	<b>(16.8)</b>	<b>12.9</b>	<b>(13.1)</b>	<b>16.2</b>	<b>15.6</b>	<b>15.6</b>	<b>15.9</b>	<b>17.9 ± 1.0</b>

<sup>a</sup> In kcal/mol; bold type (in product rows) shows the reaction enthalpy at 298 K. <sup>b</sup> PMP2/6-31G\*\*//MP2/6-31G\*\* energy with ZPE calculated using either the unscaled MP2/6-31G\*\* frequencies (first column) or the (U)HF/6-31G\*\* frequencies scaled by 0.8929 (second column in brackets). <sup>c</sup> MP4SDTQ/6-31G\*\*//MP2/6-31G\*\* energy with ZPE as above. <sup>d</sup> Calculated using the enthalpies of formation from refs 5 and 15.

energies. These tables also include the calculated reaction enthalpy values at room-temperature derived from calculated vibrational frequencies and rotational constants. Experimental values of reaction enthalpies are obtained using the most recent estimated enthalpy of formation of reactants and products. The estimation of the formation enthalpy of both radicals, CH<sub>2</sub>OH and CH<sub>3</sub>O are known with a precision not better than ±1 kcal/mol.<sup>5,15</sup> Therefore, possible differences of ±2 kcal/mol from the experimental value can be considered as acceptable.

**CH<sub>3</sub>OH + Cl Reaction.** Overall calculated values of reaction enthalpy for both channels of the CH<sub>3</sub>OH + Cl reaction are in very good agreement with the experimental value. The best values are those obtained at the G2, G2MP2, and G2MP3 levels, showing that G2MP2 is sufficient to obtain good energetics. The most stable structure for CH<sub>3</sub>OH + Cl reaction system is the molecular complex MC2, the stabilization energy of which is 10 kcal/mol below the reactants at G1, G2, and MP2 levels. Inclusion of the zero-point energies leads to an energy of the transition state TS2a lower than the one of the molecular complex MC2a. Then, the unstable MC2a molecule undergoes isomerization to MC2 without energy barrier. Thus, MC2a and TS2a, which seem to appear in the reaction mechanism, in fact do not play any role in the reaction kinetics. Thermal stability of the two other complexes (MC1 and MC2) with respect to the final channel products is estimated at 4 kcal/mol for any method including electron correlation energy. Differences are observed for the estimations of energy barrier heights, i.e., energy of transition states TS1 and TS2. G1 and G2 methods predict the location of TS1 (methoxy channel) at about 8 kcal/mol above the reactant energy, whereas at the MP2 and MP4 levels this energy barrier is higher by 3.0 kcal/mol. Larger

energy differences are obtained for TS2. PMP2 and PMP4 energies are very close to reactant energy, while G1 and G2 methods locate TS2 about 5 kcal/mol below. The molecular complex MC3 is located 5 kcal/mol below the reactants. A slightly lower thermal stability of MC3 is predicted by the MP2 and MP4 methods.

As in the case of the CH<sub>3</sub>OH + F reaction, the mechanism of the hydrogen abstraction from methanol by chlorine atoms is quite complex. The energy profile obtained at the G2 level is shown in Figure 3. In the first elementary step, attack of the chlorine atom either on the methyl side or on the hydroxyl side of CH<sub>3</sub>OH leads to the formation of a loose molecular complex, MC3, which may yield both R1 and R2 channel products. Due to the lack of thermal stability of MC2a, the next elementary step for the R2 reaction channel leads, via TS2 (with a very low energy barrier of 0.1 kcal/mol), directly to the molecular complex MC2, which dissociates to the final channel products. The reaction pathway, which yields the methoxy channel products (R1) first forms a molecular complex, MC3, goes through a transition state TS1 toward another molecular complex, MC1, which finally dissociates into the methoxy radical and HCl. There is a possibility for another pathway concerning the hydroxyl side attack of chlorine atom, which, starting directly from completely separated reactants, leads, via transition state TS1 to MC1 and next to the methoxy products. Optimized structure of this saddle point is very close to the TS1 optimized structure (except for conservation of a C<sub>s</sub> symmetry) and its Hessian matrix possesses two negative eigenvalues with both eigenvectors corresponding to a motion of the hydrogen atom between oxygen and chlorine atoms.

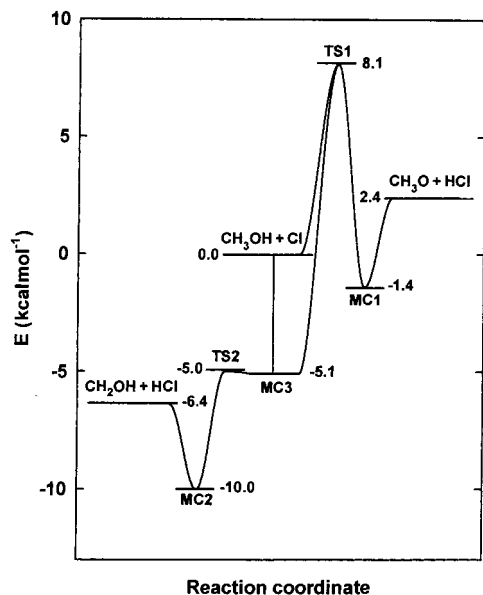


**Figure 3.** Schematic energy profile for  $\text{CH}_3\text{OH} + \text{Cl}$  reaction. The energies are calculated at the G2 level including zero-point energy corrections.

Therefore formation of the methoxy channel products may proceed by two possible ways.

**$\text{CH}_3\text{OH} + \text{Br}$  Reaction.** Owing to the difficulties with SCF convergence using the 6-311G\*\* basis set, the results are those calculated at MP2 and MP4 levels using 6-31G\* basis set. Hopefully, even with this basis set the calculated reaction enthalpies, especially those derived from MP2 calculations, are in quite satisfactory agreement with experimental ones. It is interesting to note that reaction enthalpies calculated at the G2 level are worse than PMP2 ones for both reaction channels. As the PMP2 results give the best agreement with experimental enthalpies, we have chosen this result as reference for the next rate constant calculation. The MC6 molecular complex lies 6.8 kcal/mol below the reactants at PMP2 and PMP4 levels. Good agreement between PMP2 and PMP4 results was also reached for TS4 and almost as good for TS3. However, differences in thermal stability of molecular complexes, MC4 and MC5, obtained at both levels of theory are greater (ca. 2 kcal/mol between PMP2 and PMP4). Thermal stability of MC4 with respect to the methoxy channel products is estimated to be around 4.8 kcal/mol at PMP2 and PMP4 levels. At the MP2 and MP4 levels the molecular complex MC5 is located 5.0 kcal/mol below the hydroxymethyl channel products. The heights of energy barrier of 6.5 and 19.0 kcal/mol for TS4 and TS3, respectively, suggest that formation of hydroxymethyl should be the dominant reaction channel. The molecular complex MC5a is unstable after including the zero-point vibrational energy. Its total energy is slightly higher than TS4a so that both structures, MC5a and TS4a only seemingly take part in the reaction kinetics. This is in line with the unstable molecular complex MC2a found in the  $\text{CH}_3\text{OH} + \text{Cl}$  reaction system. The energy profile for the  $\text{CH}_3\text{OH} + \text{Br}$  reaction system is shown in Figure 4. Both transition states TS3 and TS4 are located significantly above reactant energy. As for the reaction  $\text{CH}_3\text{OH} + \text{Cl}$ , occurrence of bound complexes implies a complex mechanism for the kinetics of the reaction of methanol with bromine. Indeed, for any reaction channel there are two possible pathways: with and without formation of MC6 as the first elementary step. For instance, formation of hydroxymethyl radicals (channel R4) may proceed by the following pathway:  $\text{CH}_3\text{OH} + \text{Br} \leftrightarrow \text{MC6} \leftrightarrow \text{MC5} \rightarrow \text{CH}_2\text{OH} + \text{HBr}$  and  $\text{CH}_3\text{OH}$

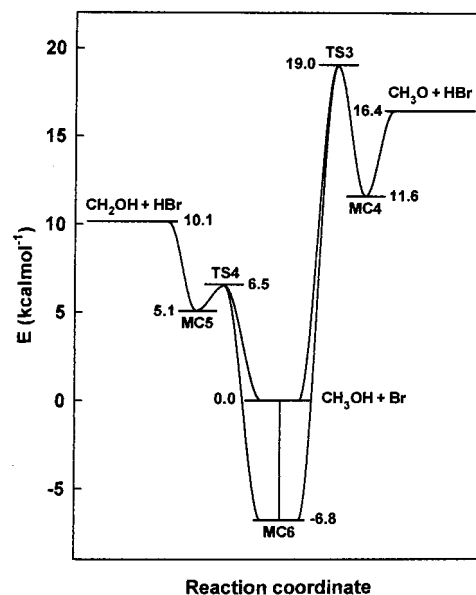


**Figure 4.** Schematic energy profile for  $\text{CH}_3\text{OH} + \text{Br}$  reaction. The energies are calculated at the PMP2/6-31G\* level including zero-point energy corrections.

$+ \text{HBr} \leftrightarrow \text{MC5} \rightarrow \text{CH}_2\text{OH} + \text{HBr}$ , whereas methoxy radicals (channel R3) are formed in the reactions  $\text{CH}_3\text{OH} + \text{Br} \leftrightarrow \text{MC6} \leftrightarrow \text{MC4} \rightarrow \text{CH}_3\text{O} + \text{HBr}$  and  $\text{CH}_3\text{OH} + \text{Br} \leftrightarrow \text{MC4} \rightarrow \text{CH}_3\text{O} + \text{HBr}$ . Rate constants for both reaction channels can be evaluated on the basis of a RRKM-like method.

### 3. Calculation of Rate Constants

**3.1. Method Used.** In part 1<sup>6</sup> we derived a general expression for a rate constant in the case of a bimolecular reaction in which two intermediate complexes are formed. Accordingly, the rate constant for the formation of hydroxymethyl (channel R2) by  $\text{CH}_3\text{OH} + \text{Cl}$  reaction system can be written as

$$k_{R2} = \frac{z}{hQ_A Q_B} \int_0^\infty dE \sum_{J=0}^{J_m} \sum_{K=0}^{K_m} W_3(E, J, K) \times \frac{W_2^*(E, J, K)}{W_3(E, J, K) + W_2^*(E, J, K) + W_1^*(E, J, K)} \times \frac{W_2(E, J, K)}{W_2(E, J, K) + W_2^*(E, J, K)} \exp(-E/RT) \quad (1)$$

where (i)  $Q_A$  and  $Q_B$  are the partition functions of  $\text{CH}_3\text{OH}$  and  $\text{Cl}$  with the center of mass translational partition function factored out of the product  $Q_A Q_B$ , and included in  $z$ . (ii)  $W_i(E, J, K)$  denotes the sum of states at energy less than or equal to  $E$ , and at angular momentum quantum numbers  $J$  and  $K$ , for transition states (denoted by a \*) and "activated complexes" for unimolecular dissociation of the respective molecular complexes. Index  $i$  labels transition states (TS $i$ ) and molecular complexes (MC $i$ ) according to the notation in Figure 3. (iii) The bottom limit of the integral is given by the threshold energy of the reaction. It is equal to zero for the hydroxymethyl formation R2 because all characteristic points of the potential energy surface for this reaction channel (MC3, TS2, MC2, and products) are located below the reactant energy level (see Figure 3). If  $V_i(0)$  denotes the potential energy of the transition state/activated complex at the angular momentum  $J = 0$ , and  $U_i(J, K)$

is its rotational energy corresponding to angular momentum quantum numbers  $J$  and  $K$ , then the upper limit  $J_m$  at given  $E$  is given by following conditions:

$$J_m(E) = \min_i \{J_i\} \quad (2)$$

where  $J_i$  is the highest integer satisfying the inequality

$$V_i(0) + U_i(J_i, 0) \leq E \quad (3)$$

and index  $i$  runs through all the transition states/activated complexes for the reaction pathway under investigation. At fixed  $E$  and  $J$ , the upper limit of  $K$ ,  $K_m$  is determined by

$$K_m(E, J) = \min_i \{K_i\} \quad (4)$$

with  $K_i$  given by the conditions:

$$V_i(0) + U_i(J, K_i) \leq E \quad \text{and} \quad K_i \leq J \quad (5)$$

The sum of states  $W(E, J, K)$  is calculated using the classical harmonic-oscillator and rigid-rotor approximation. Rotational energy at given angular momentum ( $J, K$ ) is derived for an assumed prolate symmetry top system. We also assume that the geometry of the transition states does not depend on energy and angular momentum. The simplified version of the statistical adiabatic channel model (SSACM) developed by Troe<sup>16</sup> is used to derive structural parameters of activated complex, i.e., the centrifugal energy barriers, and quanta of the “disappearing” and “conserved” oscillators. The sum of the vibrational states necessary for calculation of  $W(E, J, K)$  has been evaluated by inverse Laplace transformation of respective partition functions using the steepest descent method.<sup>17</sup> All computational details related to calculation of rate constant and the method used for description of unimolecular processes are discussed in our part 1.<sup>6</sup>

**3.2. Rate constants for CH<sub>3</sub>OH + Cl Reaction.** As is shown in Figure 3, the reaction pathway which leads to the formation of hydroxymethyl is characterized by the very small (below 0.1 kcal/mol) energy barrier of TS2. The structural parameters at the G2 level (scaled by 0.8929 vibrational frequencies obtained in SCF/6-31G\* calculation and rotational constants from MP2/6-31G\* optimized geometry) were used for molecules which participate in the reaction. It was shown in part I that calculation of the sum of states for activated complexes in the SSACM approach requires the evaluation of two empirical parameters: the “looseness” parameter  $\alpha$  and the Morse parameter  $\beta$ , which describes the potential energy along the dissociation path.<sup>16</sup> The value of the Morse parameter  $\beta$  is usually derived from the energy of the vibrational mode  $\epsilon_{RC}$ , corresponding to the bond which will break and which is often called the “reaction coordinate”, as

$$\beta = \frac{\pi}{h} \epsilon_{RC} \sqrt{\frac{2\mu}{D}} \quad (6)$$

with  $D$  the dissociation energy and  $\mu$  the reduced mass of the fragments. The “looseness” parameter  $\alpha$  is in general considered as a fitted parameter, the value of which is chosen to get the best agreement with experiment. However, comparative studies for a wide group of unimolecular reactions show that optimal choice of the  $\alpha$  value should correspond to the ratio of  $\alpha/\beta$  close to 0.5 (the value of  $0.46 \pm 0.07$  is recommended by Cobos and Troe,<sup>18</sup> and this ratio is used in our calculation for the estimation of  $\alpha$  for all unimolecular processes). As in the

case of the CH<sub>3</sub>OH + F reaction, the energy  $\epsilon_{RC}$  of the oscillator corresponding to the reaction coordinate is related to  $\nu_3$ , the vibrational frequency of all the intermediate complexes (MC1, MC2, and MC3). Then, the separation of vibrational modes of molecular complexes into two classes, the “disappearing” and “conserved” oscillators, was easily carried out. The complexes are very loose, and it is apparent from the tables concerning the structural parameters that the frequencies higher than  $\nu_4$  (in MC3) and  $\nu_6$  (in MC1, MC2) are indeed identical or very close to the vibrational modes of isolated CH<sub>3</sub>OH, CH<sub>2</sub>OH, CH<sub>3</sub>O, and HCl molecules. All internal parameters of the SSACM method used were determined by the molecular parameters derived from ab initio calculation, and there is no fitting or adjustable parameter.

A choice of the G2 molecular parameters for the rate constant calculation, however significantly overestimates both the value of the calculated rate constant and its dependence on temperature. For the hydroxymethyl channel R2, we obtained values of the rate constant of  $1.2 \times 10^{-10}$  and  $2.5 \times 10^{-10}$  cm<sup>3</sup> molecule<sup>-1</sup> s<sup>-1</sup> at 300 and 500 K, respectively. Our room temperature value is then almost two times greater than the one estimated experimentally<sup>3</sup> ( $5.1\text{--}6.3$ )  $\times 10^{-11}$  cm<sup>3</sup> molecule<sup>-1</sup> s<sup>-1</sup>. There are no direct experimental data at higher temperature, but some information can be extracted from available direct measurements for the reverse reaction CH<sub>2</sub>OH + HCl  $\rightarrow$  CH<sub>3</sub>OH + Cl. Results of Dóbbé et al.<sup>3e</sup> lead via the equilibrium constant to a value of the rate constant for the R2 channel of  $6.6 \times 10^{-11}$  cm<sup>3</sup> molecule<sup>-1</sup> s<sup>-1</sup> at 500 K. It is considerably less than our value even if the possible uncertainties in equilibrium constant related to value of the enthalpy of formation for hydroxymethyl radical are taken into account. On the other hand, unimolecular recombination is usually characterized by activation energy close to zero, which implies only weak temperature dependence of rate constants. The estimated rate constant for the first elementary step CH<sub>3</sub>OH + Cl  $\rightarrow$  MC3 also depends strongly on temperature. Troe’s method applied to this type of reactions usually gives reasonable results. Possible explanation of the anomalous temperature dependence of the calculated rate constant is due to uncertainties in the molecular parameters used. This was previously observed for the rate constant calculation in the CH<sub>3</sub>OH + F reaction system. A critical molecular structure for the rate constant calculation is, of course, the molecular complex MC3. It is a very loose complex with distances between chlorine atom and the nearest contact atoms greater than 2.5 Å at MP2/6-31G\* level and therefore this leads to very low values for the three lowest vibrational frequencies. The most sensitive model parameters are the lowest frequencies, because they correspond to the three disappearing oscillators. Among them, one is representative of the vibration of the reaction coordinate and therefore gives the value of the Morse parameter  $\beta$ . The lowest frequencies obtained at the MP2/6-31G\* level are considerably more realistic, and if they are used in the calculation of the rate constants of CH<sub>3</sub>OH + Cl reaction, they allow a satisfactory description of its kinetics. On the other hand, the scaled SCF/6-31G\* frequencies used in G2 approach give a correct estimation of the zero-point energy, so that the calculated total energies at 0 K are probably well estimated and should be conserved. Therefore, for each molecular structure, we have used the individual scaling factor, which reproduces best the ZPE value as in standard G2 calculations. Indeed, all scaling factors derived in this way are close to 0.94 ( $\pm 0.015$ ).

Use of the scaled MP2/6-31G\* frequencies leads to an increase in the values of the Morse parameters  $\beta$ , and lowers



**TABLE 5: Calculated Rate Constants for the Formation of Hydroxymethyl,  $k_{\text{Cl}}(\text{CH}_2\text{OH})$ , Methoxy Radicals,  $k_{\text{R1}}$ ,  $k'_{\text{R1}}$  and  $k_{\text{Cl}}(\text{CH}_3\text{O})$ , and the Overall Rate Constant,  $k_{\text{ov}}$  for the  $\text{CH}_3\text{OH} + \text{Cl}$  Reaction**

$T$ (K)	$k_{\text{Cl}}(\text{CH}_2\text{OH})$ ( $\text{cm}^3 \text{ molecule}^{-1} \text{ s}^{-1}$ )	$k_{\text{R1}}^a$ ( $\text{cm}^3 \text{ molecule}^{-1} \text{ s}^{-1}$ )	$k'_{\text{R1}}^b$ ( $\text{cm}^3 \text{ molecule}^{-1} \text{ s}^{-1}$ )	$k_{\text{Cl}}(\text{CH}_3\text{O})^c$ ( $\text{cm}^3 \text{ molecule}^{-1} \text{ s}^{-1}$ )	$k_{\text{ov,calcd}}$ ( $\text{cm}^3 \text{ molecule}^{-1} \text{ s}^{-1}$ )	$k_{\text{ov,exptl}}$ ( $\text{cm}^3 \text{ molecule}^{-1} \text{ s}^{-1}$ )
300	$7.08 \times 10^{-11}$	$4.08 \times 10^{-19}$	$6.92 \times 10^{-18}$	$7.32 \times 10^{-18}$	$7.1 \times 10^{-11}$	$(5.3-6.3) \times 10^{-11}$ <sup>d</sup>
400	$6.99 \times 10^{-11}$	$1.83 \times 10^{-17}$	$3.01 \times 10^{-16}$	$3.19 \times 10^{-16}$	$7.0 \times 10^{-11}$	
500	$6.91 \times 10^{-11}$	$2.06 \times 10^{-16}$	$3.28 \times 10^{-15}$	$3.48 \times 10^{-15}$	$6.9 \times 10^{-11}$	$6.6 \times 10^{-11}$ <sup>e</sup>
600	$6.83 \times 10^{-11}$	$1.13 \times 10^{-15}$	$1.75 \times 10^{-14}$	$1.87 \times 10^{-14}$	$6.8 \times 10^{-11}$	
700	$6.77 \times 10^{-11}$	$4.09 \times 10^{-15}$	$6.17 \times 10^{-14}$	$6.58 \times 10^{-14}$	$6.8 \times 10^{-11}$	
1000	$6.74 \times 10^{-11}$	$5.11 \times 10^{-14}$	$7.23 \times 10^{-13}$	$7.74 \times 10^{-13}$	$6.8 \times 10^{-11}$	

<sup>a</sup> The rate constant for the reaction:  $\text{CH}_3\text{OH} + \text{Cl} \rightleftharpoons \text{MC3} \rightleftharpoons \text{MC1} \rightarrow \text{CH}_3\text{O} + \text{HCl}$ . <sup>b</sup> The rate constant for the reaction:  $\text{CH}_3\text{OH} + \text{Cl} \rightleftharpoons \text{MC1} \rightarrow \text{CH}_3\text{O} + \text{HCl}$ . <sup>c</sup>  $k_{\text{Cl}}(\text{CH}_3\text{O}) = k_{\text{R1}} + k'_{\text{R1}}$ . <sup>d</sup> From ref 3. <sup>e</sup> Estimated value from ref 3f.

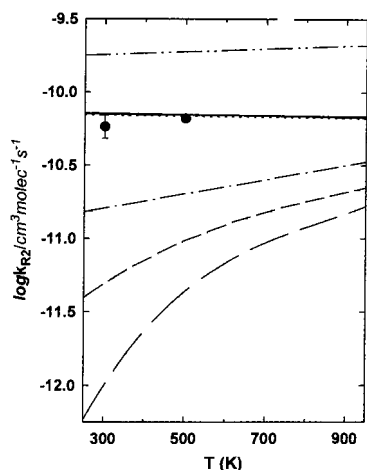


**Figure 5.** The rate constants,  $k_{\text{Cl}}(\text{CH}_2\text{OH})$  measured experimentally<sup>3</sup> (symbols) and calculated at different levels of theory (lines) from molecular parameters obtained by G2 method with scaled SCF/6-31G\* frequencies (• - •), G2 with scaled MP2/6-31G\* frequencies (solid line), G2 with scaled MP2/6-311G\*\* frequencies (dotted line), PMP2/6-311G\*\* with frequencies as above (• -), MP4SDTQ/6-311G\*\*//MP2/6-311G\*\* with frequencies as above (short dashed line), PMP2/6-31G\* with scaled MP2/6-31G\* frequencies (long dashed line).

the rate constants by a factor of almost 2. Results of calculation of the rate constants for hydroxymethyl reaction channel are given in Table 5. Value of calculated  $k_{\text{R2}}$  at room temperature is of  $7.1 \times 10^{-11} \text{ cm}^3 \text{ molecule}^{-1} \text{ s}^{-1}$ , and a very weak negative dependence on temperature is derived. This was expected, as the potential energy surface presents an association reaction followed by an almost zero energy barrier for decomposition. The calculated rate constant for the formation of hydroxymethyl radicals  $k_{\text{Cl}}(\text{CH}_2\text{OH})$  can be expressed in the temperature range 300–1000 K as

$$k_{\text{Cl}}(\text{CH}_2\text{OH}) = 6.6 \times 10^{-11} \exp(23/T) \text{ cm}^3 \text{ molecule}^{-1} \text{ s}^{-1} \quad (7)$$

Results of direct measurements<sup>3</sup> of  $k_{\text{R2}}$  are  $(5.3-6.3) \times 10^{-11} \text{ cm}^3 \text{ molecule}^{-1} \text{ s}^{-1}$  at room temperature. Our calculated value should be considered as very close to the experimental estimation. It is important to note that unimolecular processes were analyzed in the high-pressure limit approach, so that values of the calculated rate constant can be higher than observed in intermediate pressure range. However, a possible pressure-dependence of the rate constant was neither considered nor analyzed experimentally.

A comparison of the rate constant,  $k_{\text{R2}}$  calculated from molecular parameters obtained at different levels of theory are shown in Figure 5. The height of the energy barrier at the second elementary step determines the values of rate constants and their dependence on temperature. Therefore, using the molecular properties of the structures obtained at MP2/6-31G\*,

MP2/6-311G\*\*, and MP4/6-311G\*\*//MP2/6-311G\*\* levels leads to markedly lower values of the rate constants compared to those obtained at the G2 level. On the other hand, results derived from G2 molecular parameters show that the values of rate constants are quite sensitive to the choice of the vibrational frequencies used in the calculations. Using the set of MP2 frequencies (scaled by 0.94 for both basis sets) leads to rate constants which reproduce very well the available experimental findings. A good quantitative agreement between values of experimental and calculated rate constants calculated using this approach was also achieved for the  $\text{CH}_3\text{OH} + \text{F}$  reaction system previously studied.<sup>6</sup> Therefore we can conclude that the choice of molecular parameters based on the G2 energies and scaled MP2 frequencies enables one to obtain realistic description of the reacting system.

Results of direct measurements of the reverse reaction  $\text{CH}_2\text{-OH} + \text{HCl} \rightarrow \text{CH}_3\text{OH} + \text{Cl}$  leads, via the equilibrium constant, to  $k_{\text{R2}}$  of  $6.6 \times 10^{-11} \text{ cm}^3 \text{ molecule}^{-1} \text{ s}^{-1}$  at 500 K.<sup>3e</sup> This confirms the very weak dependence on temperature of  $k_{\text{R2}}$ , and is in agreement with our theoretical results.

As we described previously, formation of methoxy radicals may proceed using two competing reaction pathways, with ( $k_{\text{R1}}$ ) or without ( $k'_{\text{R1}}$ ) formation of molecular complex MC3 at the first elementary step. The corresponding rate constants are calculated as follows

$$k_{\text{R1}} = \frac{z}{hQ_{\text{A}}Q_{\text{B}}} \int_{v_{\text{T}}^{\ddagger}(0)}^{\infty} dE \sum_{J=0}^{J_m} \sum_{K=0}^{K_m} W_3(E, J, K) \times \frac{W_1^*(E, J, K)}{W_3(E, J, K) + W_2^*(E, J, K) + W_1^*(E, J, K)} \times \frac{1}{W_1(E, J, K) + W_1^*(E, J, K)} \exp(-E/RT) \quad (8)$$

$$k'_{\text{R1}} = \frac{z}{hQ_{\text{A}}Q_{\text{B}}} \int_{v_{\text{T}}^{\ddagger}(0)}^{\infty} dE \sum_{J=0}^{J_m} \sum_{K=0}^{K_m} W_1^*(E, J, K) \times \frac{1}{W_1(E, J, K) + W_1^*(E, J, K)} \quad (9)$$

with the same meaning for the symbols as in eq 1. At any energy state labeled by  $(E, J, K)$ , the expression under integrals of sums (eqs 8 and 9) is less than  $W_1^*(E, J, K)$ , so that

$$k_{\text{R1}} + k'_{\text{R1}} < \frac{2z}{hQ_{\text{A}}Q_{\text{B}}} \int_{v_{\text{T}}^{\ddagger}(0)}^{\infty} dE \sum_{J=0}^{J_m} \sum_{K=0}^{K_m} W_1^*(E, J, K) \exp(-E/RT) \quad (10)$$

Evaluation of integral 10 is standard. It is equal to the partition function of all degrees of freedom included in  $W_1^*(E, J, K)$  multiplied by  $RT \exp[-V_1^*(0)/RT]$ . Then, the right side of eq 10 is equal to  $2k_{\text{TS1}}$ , where  $k_{\text{TS1}}$  is the rate constant calculated on the basis of transition state theory for TS1 in the absence of intermediate complexes. Therefore, the upper limit of the rate constant related to the formation of the methoxy radical,  $k_{\text{Cl}}(\text{CH}_3\text{O}) = k_{\text{R1}} + k'_{\text{R1}}$  is given by  $2k_{\text{TS1}}$ .

As shown in Table 5 the calculated rate constant  $k_{\text{Cl}}(\text{CH}_3\text{O})$  for the formation of methoxy radicals is a few orders of magnitude lower than for the hydroxymethyl channel. In the temperature range 300–1000 K, the rate constant,  $k_{\text{Cl}}(\text{CH}_3\text{O})$  can be shown as

$$k_{\text{Cl}}(\text{CH}_3\text{O}) = 1.5 \times 10^{-12} \times (T/300)^{2.5} \exp(-3665/T) \text{ cm}^3 \text{ molecule}^{-1} \text{ s}^{-1} \quad (11)$$

According to the high energy barrier on the way to formation of  $\text{CH}_3\text{O}$ ,  $k_{\text{Cl}}(\text{CH}_3\text{O})$  strongly depends on temperature. However, even at 1000 K the hydroxymethyl branching fraction is close to unity. Values of the overall rate constant,  $k_{\text{ov}}$  decreases weakly when temperature increases, and from 600 K up are stabilized with a value of  $6.8 \times 10^{-11} \text{ cm}^3 \text{ molecule}^{-1} \text{ s}^{-1}$ . The calculated branching ratio values for  $\text{CH}_2\text{OH}$  formation are in agreement with the one measured experimentally, if the experimental error limits are taken into account. However, it should be noted that there are only small differences in energy barriers for  $\text{MC2} \rightarrow \text{CH}_2\text{OH} + \text{HCl}$  and  $\text{MC2} \rightarrow \text{MC3}$ , at the last elementary step for hydroxymethyl reaction pathway. At higher temperatures, an equilibrium concentration of MC2 should be observed. As a consequence, decay of the reactants does not correspond exactly to the concentration of the formed hydroxymethyl, because a part of the reactants which undergoes reaction is “frozen” as MC2. Therefore, the measurements of the branching fraction of hydroxymethyl may underestimate the efficiency of formation of  $\text{CH}_2\text{OH}$ . Our theoretical branching ratio values indicate that hydrogen abstraction from the hydroxyl site of methanol is nearly inactive at temperature below 1000 K.

The temperature dependence of the rate constant calculated for the  $\text{CH}_3\text{OH} + \text{Cl}$  reactions,  $k_{\text{Cl}}(\text{CH}_2\text{OH})$  and  $k_{\text{Cl}}(\text{CH}_3\text{O})$  cannot be examined because of a lack of direct measurements at temperatures higher than ambient. However, there are available results of kinetic measurements obtained for the reverse reaction,  $\text{CH}_2\text{OH} + \text{HCl} \rightarrow \text{CH}_3\text{OH} + \text{Cl}$  (–R2) in the temperature range 500–1000 K. Realistic estimation of the reaction enthalpy for both reaction channels obtained at G2 level allows an evaluation of the rate constants for reverse reactions (–R1, –R2) via theoretically derived equilibrium constants. The rate constants calculated in this way are given in Table 6 for  $\text{CH}_3\text{O} + \text{HCl}$  ( $\text{CH}_3\text{OH} + \text{Cl}$  (–R1) and  $\text{CH}_2\text{OH} + \text{HCl}$  ( $\text{CH}_3\text{OH} + \text{Cl}$  (–R2) and can be expressed in the form

$$k_{-\text{R1}} = 2.7 \times 10^{-14} \times (T/300)^{2.5} \exp(-2230/T) \text{ cm}^3 \text{ molecule}^{-1} \text{ s}^{-1} \quad (12a)$$

$$k_{-\text{R2}} = 5.8 \times 10^{-13} \exp(-2760/T) \text{ cm}^3 \text{ molecule}^{-1} \text{ s}^{-1} \quad (12b)$$

Calculated values of  $k_{-\text{R1}}$  and  $k_{-\text{R2}}$  are determined either by the heights of energy barriers or reaction energetics. The first reaction (–R1) is weakly exothermic (–2.4 kcal/mol at 0 K). The rate constants for H-abstraction from HCl by hydroxymethyl and methoxy radicals are close to each other, with values at

**TABLE 6: Calculated Rate Constants for the Reverse Reactions:  $\text{CH}_3\text{O} + \text{HCl} \rightarrow \text{CH}_3\text{OH} + \text{Cl}$  ( $k_{-\text{R1}}$ ) and  $\text{CH}_2\text{OH} + \text{HCl} \rightarrow \text{CH}_3\text{OH} + \text{Cl}$  ( $k_{-\text{R2}}$ )**

$T$ (K)	$K_1^a$	$k_{-\text{R1}}^b$ ( $\text{cm}^3$ $\text{molecule}^{-1} \text{ s}^{-1}$ )	$K_2^c$	$k_{-\text{R2}}^d$ ( $\text{cm}^3$ $\text{molecule}^{-1} \text{ s}^{-1}$ )
300	$4.54 \times 10^{-1}$	$1.61 \times 10^{-17}$	$1.24 \times 10^6$	$5.69 \times 10^{-17}$
400	1.48	$2.16 \times 10^{-16}$	$1.13 \times 10^5$	$6.20 \times 10^{-16}$
500	3.04	$1.14 \times 10^{-15}$	$2.80 \times 10^4$	$2.47 \times 10^{-15}$
600	4.94	$3.79 \times 10^{-15}$	$1.13 \times 10^4$	$6.04 \times 10^{-14}$
700	6.97	$9.44 \times 10^{-15}$	$5.98 \times 10^3$	$1.13 \times 10^{-14}$
1000	$1.27 \times 10^1$	$6.09 \times 10^{-14}$	$1.90 \times 10^3$	$3.54 \times 10^{-14}$

<sup>a</sup> The equilibrium constant for the reaction:  $\text{CH}_3\text{OH} + \text{Cl} \rightleftharpoons \text{CH}_3\text{O} + \text{HCl}$ . <sup>b</sup> The rate constant for the reaction:  $\text{CH}_3\text{O} + \text{HCl} \rightarrow \text{CH}_3\text{OH} + \text{Cl}$ . <sup>c</sup> The equilibrium constant for the reaction:  $\text{CH}_3\text{OH} + \text{Cl} \rightleftharpoons \text{CH}_2\text{OH} + \text{HCl}$ . <sup>d</sup> The rate constant for the reaction:  $\text{CH}_2\text{OH} + \text{HCl} \rightarrow \text{CH}_3\text{OH} + \text{Cl}$ .

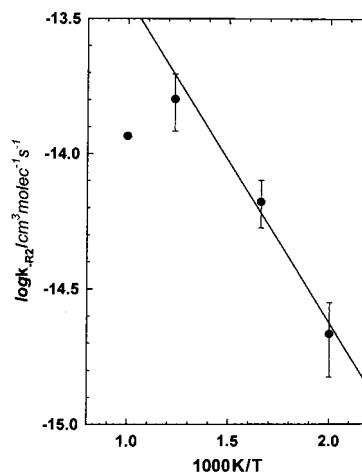


**Figure 6.** Arrhenius plot for the  $\text{CH}_2\text{OH} + \text{HCl} \rightarrow \text{CH}_3\text{OH} + \text{Cl}$  reaction (–R2) comparing results of this study obtained on the basis of eq 12b (line) with kinetic measurements (symbols) of Dóbe et al.<sup>3e</sup>

300 K of  $1.6 \times 10^{-17} \text{ cm}^3 \text{ molecule}^{-1} \text{ s}^{-1}$  and  $6.0 \times 10^{-17} \text{ cm}^3 \text{ molecule}^{-1} \text{ s}^{-1}$  for  $k_{-\text{R1}}$  and  $k_{-\text{R2}}$ , respectively. However, the rate constant for the  $\text{CH}_3\text{O} + \text{HCl}$  reaction,  $k_{-\text{R1}}$  increases more than  $k_{-\text{R2}}$  when the temperature rises.

In Figure 6 is shown an Arrhenius plot for  $\text{CH}_2\text{OH} + \text{HCl} \rightarrow \text{CH}_3\text{OH} + \text{Cl}$  reaction in the temperature range of 500–1000 K. The values of the rate constant  $k_{-\text{R2}}$  derived from eq 12 are in very good agreement with experiments. Only the experimental point at 1000 K deviates from the theoretical line. However, its value is significantly underestimated compared to the other experiments at lower temperatures. The exact value of  $k_{-\text{R2}}$  is not known at room temperature. An approximate estimation of  $k_{-\text{R2}}$  lower than  $5 \times 10^{-16} \text{ cm}^3 \text{ molecule}^{-1} \text{ s}^{-1}$  given by Dóbe et al.<sup>3f</sup> is in line with our calculated value of  $6 \times 10^{-17} \text{ cm}^3 \text{ molecule}^{-1} \text{ s}^{-1}$  at 300 K. The quantitative agreement between theoretical and measured values of  $k_{-\text{R2}}$  obtained over a wide range of temperature confirms also the good representation of the temperature dependence of the rate constant for the primary reaction  $\text{CH}_3\text{OH} + \text{Cl} \rightarrow \text{CH}_2\text{OH} + \text{HCl}$ .

**3.3. Rate Constants for the  $\text{CH}_3\text{OH} + \text{Br}$  Reaction.** Due to the difficulties with the convergence of the SCF process with the 6-311G\*\* basis set, the optimized geometry of all the stationary points found on the potential energy surface for the  $\text{CH}_3\text{OH} + \text{Br}$  reaction system was derived with the 6-31G\* basis set. Results of MP2 calculations reproduce the reaction enthalpy values for both reaction channels better than those obtained at MP4 level. Therefore, these structural parameters

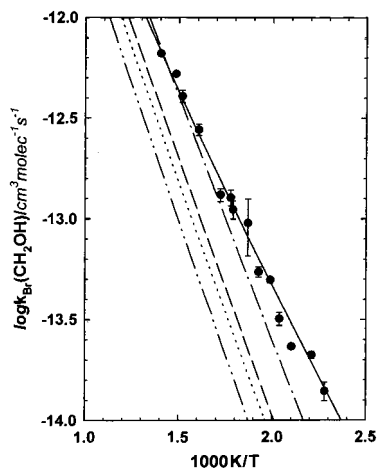


**Figure 7.** Arrhenius plot for the  $\text{CH}_3\text{OH} + \text{Br} \rightarrow \text{CH}_2\text{OH} + \text{HBr}$  reaction comparing kinetic measurements (symbols) of Dóbe et al.<sup>5</sup> with theoretical results derived on the basis of molecular parameters obtained from calculation: PMP2/6-31G\* with scaled MP2/6-31G\* frequencies (dashed line), PMP2/6-31G\* with scaled SCF/6-31G\* frequencies ( $\cdot -$ ), MP4SDTQ/6-31G\*/MP2/6-31G\* with scaled MP2/6-31G\* frequencies ( $\cdot \cdot -$ ), MP4SDTQ/6-31G\*/MP2/6-31G\* with scaled SCF/6-31G\* frequencies (dotted line). The solid line denotes recommended  $k_{\text{TS4}}$  (see text for definition).

together with the scaled (by 0.94) MP2/6-31G\* frequencies were used in the calculation of rate constants. The hydroxymethyl can be formed following two reaction pathways, with ( $k_{\text{R4}}$ ) and without ( $k'_{\text{R4}}$ ) formation of the intermediate complex MC6. Basic equations for calculation of the rate constant for total formation of hydroxymethyl,  $k_{\text{Br}}(\text{CH}_2\text{OH}) = k_{\text{R4}} + k'_{\text{R4}}$  are given by

$$k_{\text{R4}} = \frac{z}{hQ_{\text{A}}Q_{\text{B}}} \int_{V_{\text{P}}(0)}^{\infty} dE \sum_{J=0}^{J_m} \sum_{K=0}^{K_m} W_6(E, J, K) \times \frac{W_4^*(E, J, K)}{W_6(E, J, K) + W_3^*(E, J, K) + W_4^*(E, J, K)} \times \frac{W_5(E, J, K)}{W_5(E, J, K) + W_4^*(E, J, K)} \exp(-E/RT) \quad (13)$$

$$k'_{\text{R4}} = \frac{z}{hQ_{\text{A}}Q_{\text{B}}} \int_{V_{\text{P}}(0)}^{\infty} dE \sum_{J=0}^{J_m} \sum_{K=0}^{K_m} W_4^*(E, J, K) \times \frac{W_5(E, J, K)}{W_5(E, J, K) + W_4^*(E, J, K)} \quad (14)$$

where  $Q_{\text{A}}$  and  $Q_{\text{B}}$  denote the partition functions of  $\text{CH}_3\text{OH}$  and Br (with the center of mass translational partition function factored out),  $V_{\text{P}}(0)$  is the  $\text{CH}_2\text{OH}$  plus HBr channel energy at  $J = 0$  with respect to the reactant energy at 0 K, and other symbols are as in eq 1. As previously shown, the upper limit of this rate constant is given by  $2k_{\text{TS4}}$ , where  $k_{\text{TS4}}$  is the rate constant, calculated using transition state theory, for the formation of hydroxymethyl via TS4 in absence of intermediate complexes MC5 and MC6. The structural parameters necessary for the calculation of the sum of states for activated complexes are the molecular data given in Table 2.

The rate constants  $k_{\text{Br}}(\text{CH}_2\text{OH})$  calculated from molecular parameters obtained at different levels of theory are shown in Figure 7. In general the calculated rate constants are markedly

lower than the ones obtained experimentally, especially at low temperatures. Due to the fact that the MP4 energy barrier is higher by 2 kcal/mol than the MP2 one, the MP4 rate constants are significantly smaller than MP2 ones. It can also be noticed that the use of scaled SCF frequencies leads to systematically larger values of rate constants compared to those obtained on the basis of scaled MP2 frequencies. However, the largest calculated rate constants approaches those experimentally estimated only when temperature exceeds 700 K.

The values of the calculated rate constants from molecular parameters obtained at MP2/6-31G\* level are listed in Table 7. A column with values of the rate constant  $k_{\text{MC5}}$  related to overall formation of molecular complex MC5 in  $\text{CH}_3\text{OH} + \text{Br} \leftrightarrow \text{MC6} \rightarrow \text{MC5}$  and  $\text{CH}_3\text{OH} + \text{Br} \rightarrow \text{MC5}$  reactions have been added in the table. This rate constant can be derived from eqs 13 and 14 if the last fraction in the integral is replaced by unity and the lower limit of the integral by  $V_4^*(0)$ . The rate constants calculated for the formation of hydroxymethyl are significantly lower than estimated experimentally by Dóbe et al.<sup>5</sup> At 400 K, our calculated value of  $k_{\text{Br}}(\text{CH}_2\text{OH}) = k_{\text{R4}} + k'_{\text{R4}}$  is almost 8 times lower than the experimental one. When the temperature increases, the calculated value of  $k_{\text{Br}}(\text{CH}_2\text{OH})$  approaches the experimental one; but at 700 K the derived  $k_{\text{Br}}(\text{CH}_2\text{OH})$  is still two times less than estimated experimentally. The values of  $k_{\text{MC5}}$  given in the last column, are considerably larger than either  $k_{\text{Br}}(\text{CH}_2\text{OH})$  or the experimental ones. This is a consequence of the small barrier for the back reaction of the last elementary step. This barrier of 1.4 kcal/mol is 3.6 kcal/mol lower than the relative stability energy of MC5 with respect to hydroxymethyl channel products. As a consequence, only a small part of MC5 undergoes dissociation to  $\text{CH}_2\text{OH} + \text{HBr}$  especially at lower temperatures, and therefore leads to small values of  $k_{\text{Br}}(\text{CH}_2\text{OH})$ . A comparison of  $k_{\text{MC5}}$  with  $k_{\text{Br}}(\text{CH}_2\text{OH})$  shows that only 1% and less than 30% of MC5 yields the hydroxymethyl radicals, at 300 and 1000 K, respectively. On the other hand, it is important to note that values of the rate constant,  $k_{\text{TS4}}$  (denoted by the solid line in Figure 7) are very close to those estimated experimentally. In the temperature range of 500–700 K the greatest difference does not exceed 10%. As was shown previously, the upper limit of  $k(\text{CH}_2\text{OH})$  is given by  $2k_{\text{TS4}}$ , and values of  $k_{\text{MC5}}$  are close to that at any temperature. This fact suggests that, as obtained at MP2/6-31G\* level, total energies of MC5 and/or the channel products can be overestimated. Unfortunately, we could not examine the total energy of MC5 by G2 method. The thermal stability of MC5, 5.0 kcal/mol with respect to the channel products at PMP2 level is very close to values obtained using the G2 method for corresponding structures of the  $\text{CH}_3\text{OH} + \text{Cl}$  and  $\text{CH}_3\text{OH} + \text{F}$  reaction systems. This suggests that probably total energies of both MC5 and products are overestimated and should be lowered. Results of G2 calculation (for reactants and products, only) also support this conclusion. The reaction enthalpy for this reaction channel was estimated at the G2 level as being about 3 kcal/mol less than PMP2 value, and close to the energy barrier related to TS4. As shown in Figure 2, the products  $\text{CH}_2\text{OH} + \text{HBr}$  are the most thermodynamically unstable molecular systems among the stationary point systems for the hydroxymethyl reaction channel. A shift down by 2 kcal/mol of the energy levels of MC5 and the hydroxymethyl channel products should lead to the branching ratio close to 0.5 for the formation of hydroxymethyl at the last elementary step. It may be obtained by systematic lowering of the products energy levels to get the best agreement with experiment. That approach was applied by Chen et al.<sup>19</sup> in a similar calculation of the rate constants for hydrogen abstraction



**TABLE 7: Calculated Rate Constants for the Formation of Hydroxymethyl Radicals  $k_{R4}$ ,  $k'_{R4}$ , and  $k_{Br}(CH_2OH)$  and the Rate Constants  $k_{TS4}$  and  $k_{MC5}$  (definitions below the Table) for the  $CH_3OH + Br$  Reaction**

$T$ (K)	$K_{R4}^a$ (cm <sup>3</sup> molecule <sup>-1</sup> s <sup>-1</sup> )	$k'_{R4}^b$ (cm <sup>3</sup> molecule <sup>-1</sup> s <sup>-1</sup> )	$k_{Br}(CH_2OH)^c$ (cm <sup>3</sup> molecule <sup>-1</sup> s <sup>-1</sup> )	$k_{Br}(CH_2OH)$ exptl <sup>d</sup> (cm <sup>3</sup> molecule <sup>-1</sup> s <sup>-1</sup> )	$k_{TS4}^e$ (cm <sup>3</sup> molecule <sup>-1</sup> s <sup>-1</sup> )	$k_{MC5}^f$ (cm <sup>3</sup> molecule <sup>-1</sup> s <sup>-1</sup> )
300	$2.92 \times 10^{-18}$	$3.04 \times 10^{-18}$	$5.96 \times 10^{-18}$		$2.38 \times 10^{-16}$	$4.54 \times 10^{-16}$
400	$2.99 \times 10^{-16}$	$3.17 \times 10^{-16}$	$6.16 \times 10^{-16}$	$4.8 \times 10^{-15}$	$5.95 \times 10^{-15}$	$1.15 \times 10^{-14}$
500	$5.09 \times 10^{-15}$	$5.55 \times 10^{-15}$	$1.06 \times 10^{-14}$	$4.6 \times 10^{-14}$	$4.63 \times 10^{-14}$	$8.96 \times 10^{-14}$
600	$3.48 \times 10^{-14}$	$3.93 \times 10^{-14}$	$7.41 \times 10^{-14}$	$2.1 \times 10^{-13}$	$1.99 \times 10^{-13}$	$3.80 \times 10^{-13}$
700	$1.39 \times 10^{-13}$	$1.64 \times 10^{-13}$	$3.03 \times 10^{-13}$	$6.2 \times 10^{-13}$	$5.98 \times 10^{-13}$	$1.12 \times 10^{-13}$
1000	$1.70 \times 10^{-12}$	$2.40 \times 10^{-12}$	$4.10 \times 10^{-12}$		$5.33 \times 10^{-12}$	$9.25 \times 10^{-12}$

<sup>a</sup> The rate constant for the reaction:  $CH_3OH + Br \rightleftharpoons MC6 \rightleftharpoons MC5 \rightarrow CH_2OH + HBr$ . <sup>b</sup> The rate constant for the reaction:  $CH_3OH + Br \rightleftharpoons MC5 \rightarrow CH_2OH + HBr$ . <sup>c</sup>  $k_{Br}(CH_2OH) = k_{R4} + k'_{R4}$ . <sup>d</sup> From ref 5. <sup>e</sup> The rate constant calculated on the base of transition state theory for TS4 neglecting intermediate complexes MC4 and MC6. <sup>f</sup> The overall rate constant calculated for the formation of MC5 in the reactions:  $CH_3OH + Br \rightarrow MC5$  and  $CH_3OH + Br \rightleftharpoons MC6 \rightarrow MC5$ .

from hydrocarbons by halogen atoms. However, in our case, this fitting procedure must lead to values of the rate constant,  $k_{Br}(CH_2OH)$  close to the one derived for  $k_{TS4}$ , which is in excellent agreement with experiment. Therefore, we consider  $k_{TS4}$  as the best approximation to  $k_{Br}(CH_2OH)$ , which is equivalent to assumption of the branching ratio value (expressed by the sum of states in eqs 13 and 14) of 0.5 for the dissociation of MC5 to hydroxymethyl products at any energy  $E$ . The temperature dependence of the rate constant derived by this way for the formation of hydroxymethyl channel products,  $k_{Br}(CH_2OH) = k_{TS4}$ , can be expressed in the temperature range 300–1000 K as

$$k_{Br}(CH_2OH) = 4.8 \times 10^{-12} \times (T/300)^{2.6} \exp(-2975/T) \text{ cm}^3 \text{ molecule}^{-1} \text{ s}^{-1} \quad (15)$$

Figure 7 shows a good agreement between the calculated values  $k_{Br}(CH_2OH)$  and the experimental results of Dóbé et al.<sup>5</sup>

The rate constant calculation for  $CH_3O$  reaction channel was carried out on the basis of the expressions given below for  $k_{R3}$  and  $k'_{R3}$

$$k_{R3} = \frac{z}{hQ_A Q_B} \int_{V_3^{\ddagger}(0)}^{\infty} dE \sum_{J=0}^{J_m} \sum_{K=0}^{K_m} W_6(E, J, K) \times \frac{W_3^*(E, J, K)}{W_6(E, J, K) + W_3^*(E, J, K) + W_4^*(E, J, K)} \times \frac{W_4(E, J, K)}{W_4(E, J, K) + W_3^*(E, J, K)} \exp(-E/RT) \quad (16)$$

$$k'_{R3} = \frac{z}{hQ_A Q_B} \int_{V_3^{\ddagger}(0)}^{\infty} dE \sum_{J=0}^{J_m} \sum_{K=0}^{K_m} W_3^*(E, J, K) \times \frac{W_4(E, J, K)}{W_4(E, J, K) + W_3^*(E, J, K)} \quad (17)$$

Results of this calculation are given in Table 8, and they show that the efficiency of the formation of methoxy radicals given by the rate constant  $k_{Br}(CH_3O) = k_{R3} + k'_{R3}$  can be considered as negligible. In the temperature range of 300–1000 K, this rate constant can be expressed analytically as follows

$$k_{Br}(CH_3O) = 2.7 \times 10^{-12} (T/300)^{1.9} \exp(-9825/T) \text{ cm}^3 \text{ molecule}^{-1} \text{ s}^{-1} \quad (18)$$

According to the very high energy barrier, the rate constant  $k_{Br}(CH_3O)$  depends strongly on temperature, However, the

**TABLE 8: Calculated Rate Constants for the Formation of Methoxy Radicals  $k_{R3}$ ,  $k'_{R3}$  and  $k_{Br}(CH_3O)$  for the  $CH_3OH + Br$  Reaction**

$T$ (K)	$K_{R3}^a$ (cm <sup>3</sup> molecule <sup>-1</sup> s <sup>-1</sup> )	$k'_{R3}^b$ (cm <sup>3</sup> molecule <sup>-1</sup> s <sup>-1</sup> )	$k_{Br}(CH_3O)^c$ (cm <sup>3</sup> molecule <sup>-1</sup> s <sup>-1</sup> )
300	$6.35 \times 10^{-27}$	$9.70 \times 10^{-27}$	$1.61 \times 10^{-26}$
400	$3.87 \times 10^{-23}$	$6.21 \times 10^{-23}$	$1.01 \times 10^{-22}$
500	$7.81 \times 10^{-21}$	$1.33 \times 10^{-20}$	$2.11 \times 10^{-20}$
600	$2.82 \times 10^{-19}$	$5.12 \times 10^{-19}$	$7.94 \times 10^{-19}$
700	$3.77 \times 10^{-18}$	$7.33 \times 10^{-18}$	$1.11 \times 10^{-17}$
1000	$4.37 \times 10^{-16}$	$1.05 \times 10^{-15}$	$1.49 \times 10^{-15}$

<sup>a</sup> The rate constant for the reaction:  $CH_3OH + Br \rightleftharpoons MC6 \rightleftharpoons MC4 \rightarrow CH_3O + HBr$ . <sup>b</sup> The rate constant for the reaction:  $CH_3OH + Br \rightleftharpoons MC4 \rightarrow CH_3O + HBr$ . <sup>c</sup>  $k_{Br}(CH_3O) = k_{R3} + k'_{R3}$ .

formation of  $CH_3O$  does not give a contribution to the overall rate constant even at 1000 K. This is in agreement with experiment that only formation of hydroxymethyl radicals is observed.

The derived potential energy surface permits also the calculation of the rate constants for the reverse reactions:  $CH_3O + HBr \rightarrow CH_3OH + Br$  ( $-R3$ ) and  $CH_2OH + HBr \rightarrow CH_3OH + Br$  ( $-R4$ ). Evaluation of the rate constants,  $k_{-R3}$  and  $k_{-R4}$  can be straightforwardly performed via equilibrium constants obtained theoretically from molecular parameters of reactants and products. A comparison of calculated and experimental rate constants can be made for  $CH_2OH + HBr$  reaction since there are results available for direct measurements of  $k_{-R4}$  obtained in the range of 220–473 K by Dóbé et al.<sup>5</sup>

The previous calculation of  $k_{Br}(CH_2OH)$  for H-abstraction from methanol by Br atoms shows that the total energies of the hydroxymethyl channel products obtained at PMP2/6-31G\* level are probably overestimated by about 2 kcal/mol. On the other hand, using the G2 method leads to the reaction enthalpy of 2.1 kcal/mol lower compared to the one estimated on the basis of heats of formation. Calculation of  $k_{-R4}$  requires correct values of equilibrium constants. These equilibrium constants are very sensitive to reaction energetics, and lead to a systematic overestimation (PMP2) or underestimation (G2) of the values of  $k_{-R4}$ . An improvement of the total energy of  $CH_2OH + HBr$  molecular system is then of major importance for quality of final results of the calculated rate constant,  $k_{-R4}$ . Therefore we assumed that the “correct” equilibrium constant for  $CH_3OH + Br$  ( $CH_2OH + HBr$  reaction,  $K_4$  can be shown in the form  $K_4 = K_{4,PMP2} \exp(\epsilon/RT)$ , where  $K_{4,PMP2}$  is the equilibrium constant calculated for molecular parameters derived from PMP2/6-31G\* calculation (with vibrational frequencies scaled by 0.94) and  $\epsilon$  is the shift of the total energy of  $CH_2OH + HBr$  toward the value obtained at PMP2/6-31G\* level. Value of  $\epsilon$  was found by fitting of the rate constants calculated as  $k_{-R4} = k_{Br}(CH_2OH)/K_4$  to experimental results of Dóbé et al.<sup>5</sup> The best agreement was reached for  $\epsilon = 1.8$  kcal/mol. This shift down



**TABLE 9: Calculated Rate Constants for the Reverse Reactions:  $\text{CH}_3\text{O} + \text{HBr} \rightarrow \text{CH}_3\text{OH} + \text{Br}$  ( $k_{-R3}$ ) and  $\text{CH}_2\text{OH} + \text{HBr} \rightarrow \text{CH}_3\text{OH} + \text{Br}$  ( $k_{-R4}$ )**

$T$ (K)	$K_3^a$	$k_{-R3}^b$ ( $\text{cm}^3$ $\text{molecule}^{-1} \text{s}^{-1}$ )	$K_4$ $\text{exp}(\epsilon/RT)^c$	$k_{-R4}^d$ ( $\text{cm}^3$ $\text{molecule}^{-1} \text{s}^{-1}$ )
300	$3.08 \times 10^{-11}$	$5.23 \times 10^{-16}$	$2.44 \times 10^{-5}$	$9.75 \times 10^{-12}$
400	$3.71 \times 10^{-8}$	$2.72 \times 10^{-15}$	$1.09 \times 10^{-3}$	$5.46 \times 10^{-12}$
500	$2.65 \times 10^{-6}$	$7.95 \times 10^{-15}$	$1.11 \times 10^{-2}$	$4.16 \times 10^{-12}$
600	$4.59 \times 10^{-5}$	$1.73 \times 10^{-14}$	$5.35 \times 10^{-2}$	$3.72 \times 10^{-12}$
700	$3.51 \times 10^{-4}$	$3.16 \times 10^{-14}$	$1.66 \times 10^{-1}$	$3.61 \times 10^{-12}$
1000	$1.35 \times 10^{-2}$	$1.11 \times 10^{-13}$	1.27	$4.19 \times 10^{-12}$

<sup>a</sup> The equilibrium constant for the reaction:  $\text{CH}_3\text{OH} + \text{Br} \rightleftharpoons \text{CH}_3\text{O} + \text{HBr}$ . <sup>b</sup> The rate constant for the reaction:  $\text{CH}_3\text{O} + \text{HBr} \rightarrow \text{CH}_3\text{OH} + \text{Br}$ . <sup>c</sup> The equilibrium constant for the reaction:  $\text{CH}_3\text{OH} + \text{Br} \rightleftharpoons \text{CH}_2\text{OH} + \text{HBr}$  ( $K_4$ ) with  $\epsilon = 1.8$  kcal/mol. <sup>d</sup> The rate constant for the reaction:  $\text{CH}_2\text{OH} + \text{HBr} \rightarrow \text{CH}_3\text{OH} + \text{Br}$ .

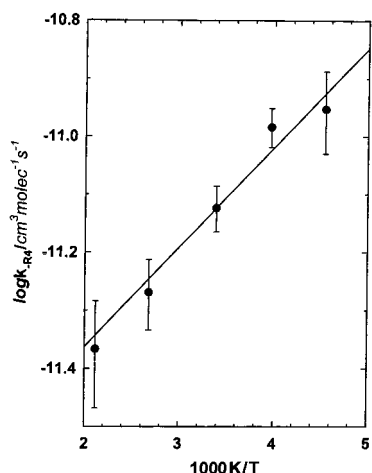


**Figure 8.** Arrhenius plot for the  $\text{CH}_2\text{OH} + \text{HBr} \rightarrow \text{CH}_3\text{OH} + \text{Br}$  reaction ( $-R4$ ) comparing results of this study obtained on the basis of eq 19b (line) with kinetic measurements (symbols) of Dóbbé et al.<sup>5</sup>

of the total energy of the  $\text{CH}_2\text{OH} + \text{HBr}$  system corresponds to the reaction enthalpy for  $\text{CH}_3\text{OH} + \text{Br} \rightarrow \text{CH}_2\text{OH} + \text{HBr}$  of 8.8 kcal/mol at 298 K, which is equal to the experimentally estimated value ( $8.8 \pm 1.0$  kcal/mol).<sup>5,15</sup>

The calculated rate constants,  $k_{-R3}$  and  $k_{-R4}$  given in Table 9 can be expressed in the form convenient for use in kinetic modeling

$$k_{-R3} = 4.1 \times 10^{-14} \times (T/300)^{1.9} \exp(-1305/T) \text{ cm}^3 \text{ molecule}^{-1} \text{ s}^{-1} \quad (19a)$$

$$k_{-R4} = 2.0 \times 10^{-12} \exp(395/T) \text{ cm}^3 \text{ molecule}^{-1} \text{ s}^{-1} \quad (19b)$$

Both reactions of H-abstraction from HBr by hydroxymethyl and methoxy radicals are exothermic. This is consistent with the fact that the values of the rate constants,  $k_{-R3}$  and  $k_{-R4}$ , are a few orders of magnitude higher than those of the corresponding primary reactions. At 300 K the resulting values of those rate constants are  $5.3 \times 10^{-16}$  and  $9.8 \times 10^{-12} \text{ cm}^3 \text{ molecule}^{-1} \text{ s}^{-1}$  for  $\text{CH}_3\text{O} + \text{HBr}$  and  $\text{CH}_2\text{OH} + \text{HBr}$  reactions, respectively. A high value of the rate constant for the hydroxymethyl reaction ( $-R4$ ) suggests an important role of this reaction for atmosphere modeling. An Arrhenius plot for  $\text{CH}_2\text{OH} + \text{HBr}$  reaction is shown in Figure 8. The complex reaction mechanism leads to a weak negative temperature dependence of the calculated values of  $k_{-R4}$ , also observed experimentally. Values of the rate constant,  $k_{-R4}$  calculated using eq 19b, are in very good agreement with experiments over a wide range of temperature.

An experimental study has been underway on the kinetics of the reaction ( $-R3$ ) in one of our laboratories.<sup>20</sup> A significantly larger rate coefficient value has been determined at room temperature. This may indicate that the barrier height of TS3 has been overestimated in the calculations.

#### 4. Conclusion

Ab initio calculations at different levels of theory were performed for the  $\text{CH}_3\text{OH} + \text{Cl}$  and  $\text{CH}_3\text{OH} + \text{Br}$  reaction system. Derived molecular properties (optimized geometries, barrier heights and vibrational levels) of the characteristic points of the potential energy surface were used to describe the mechanism of the kinetics of the reaction under investigation. Results of calculation show that the mechanism of both  $\text{CH}_3\text{OH} + \text{Cl}$  and  $\text{CH}_3\text{OH} + \text{Br}$  reactions is complex, and similar to the  $\text{CH}_3\text{OH} + \text{F}$  reaction, proceeds via the formation of intermediate complexes. However, in contrast to the previously studied  $\text{CH}_3\text{OH} + \text{F}$  reaction system, all transition states of both reactions are located above respective molecular complexes energy levels at all levels of theory.

The energy profile for the  $\text{CH}_3\text{OH} + \text{Cl}$  reaction obtained at the G2 level, indicates a very small height for the energy barrier of the hydroxymethyl reaction channel. This explains the relatively high value of the rate constant observed experimentally, significantly higher than the one expected for this almost thermoneutral reaction. The calculated rate constant for the hydroxymethyl reaction channel,  $k_{\text{Cl}}(\text{CH}_2\text{OH})$  at 300 K is in very good agreement with experimental measurements for  $\text{CH}_3\text{OH} + \text{Cl}$ . The very weak negative temperature dependence of  $k_{\text{Cl}}(\text{CH}_2\text{OH})$  obtained can be explained in terms of the relative importance of the  $\text{MC2} \rightarrow \text{MC3}$  elementary process with temperature variation. Calculated branching ratio values indicate that hydrogen abstraction from the hydroxyl-site is negligible for temperatures below 1000 K.

The reaction enthalpies for both reaction channels obtained at MP2 level for  $\text{CH}_3\text{OH} + \text{Br}$  are in good agreement with experimental estimations. However, calculation of the rate constant for hydroxymethyl reaction channel indicates that the total energies of the channel products and molecular complex MC5 are probably overestimated. Unfortunately, the total energy of MC5 estimated at MP2 level could not be checked using the G2 method owing to difficulties with convergence of the SCF process with the 6-311G\*\* basis set. Lowering total energy of both MC5 and the hydroxymethyl channel products by about 2 kcal/mol, as suggested by the results of the calculated reaction enthalpy at G2 level, should lead to the "mean" value of the branching ratio for dissociation of MC5 close to 0.5. Due to high energy barriers, this assumption corresponds to the rate constant for the R4 channel,  $k_{\text{Br}}(\text{CH}_2\text{OH})$  replaced by the rate constant calculated on the basis of conventional transition state theory via TS4 neglecting the intermediate complexes,  $k_{\text{TS4}}$ . The values of  $k_{\text{Br}}(\text{CH}_2\text{OH})$  obtained by this method are in excellent agreement with experiment. Results of the rate constant calculation for reaction channel R3 show that this channel is inactive even at the highest temperature considered in this study. It is in accordance with the sole experimentally observed formation of hydroxymethyl radicals.

Analytical expressions obtained in this study allow the successful description of kinetics of the reactions under investigation in a wide temperature range. Because of narrow temperature ranges of the experimental measurements, derived expressions are of significant importance for the chemical modeling studies.

**Acknowledgment.** This work has been performed under the auspices of European Contract "Copernicus" CIPA-CT93-0163, Chemical Kinetic Studies of Combustion related to Atmospheric Pollution. We also thank the I.D.R.I.S. Computing Center in Orsay (CNRS, France) for CPU time facilities. Part of the numerical calculations was carried out in the Wrocław Networking and Supercomputing Center (Poland).

**Supporting Information Available:** Tables of vibrational frequencies of, and optimized structures for, stationary points of the potential energy surface for  $\text{CH}_3\text{OH} + \text{Cl}$  (2 pages). Ordering information is given on any current masthead page.

## References and Notes

- (1) (a) Eyzat, P. *Rev. Assoc. Fr. Technol. Pet.* **1975**, 230, 31. (b) Aronowitz, D.; Naegell, D. W.; Glassman, I. *J. Phys. Chem.* **1977**, 81, 2555. (c) Westbrook, C. K.; Dryer, F. L. *Combust. Flame* **1980**, 37, 171. (d) Spindler, K.; Wagner, H. Gg. *Ber. Bunsen-Ges. Phys. Chem.* **1983**, 86, 2. (e) Norton, T. S.; Dryer, F. L. *Int. J. Chem. Kinet.* **1990**, 22, 219.
- (2) (a) Wallington, T. J.; Skewes, L. M.; Siegl, W. O.; Wu, C. H.; Japar, S. M. *Int. J. Chem. Kinet.* **1988**, 20, 867. (b) Nelson, L.; Rattigen, O.; Neavyn, R.; Sidebottom, H. *Int. J. Chem. Kinet.* **1990**, 22, 1111.
- (3) (a) Michael, J. V.; Nava, D. F.; Payne, W. A.; Stief, L. J. *J. Chem. Phys.* **1979**, 70, 3652. (b) Payne, W. A.; Brunning, J.; Mitchell, M. B.; Stief, L. J. *Int. J. Chem. Kinet.* **1988**, 20, 63. (c) Pagsberg, P.; Munk, J.; Sillesen, A.; Anastasi, C. *Chem. Phys. Lett.* **1988**, 146, 375. (d) Lightfoot, P. D.; Veyret, B.; Lesclaux, R. *J. Phys. Chem.* **1990**, 94, 708. (e) Dóbé, S.; Otting, M.; Temps, F.; Wagner, H. Gg.; Ziemer, H. *Ber. Bunsen-Ges. Phys. Chem.* **1993**, 97, 877. (f) 28. Dóbé, S.; Bércés, T.; Temps, F.; Wagner, H. Gg.; Ziemer, H. In *Proceedings of the 25th International Symposium on Combustion*; Combustion Institute: Pittsburgh, 1994; p 775.
- (4) (a) Buckley, E.; Whittle, E. *Trans. Faraday Soc.* **1962**, 58, 536. (b) Amphlett, J. G.; Whittle, E. *Trans. Faraday Soc.* **1964**, 64, 2130.
- (5) Dóbé, S.; Bércés, T.; Turányi, T.; Márta, F.; Grussdorf, J.; Temps, F.; Wagner, H. Gg. *J. Phys. Chem.* **1996**, 100, 19864.
- (6) Jodkowski, J. T.; Rayez, M. T.; Rayez, J. C.; Bércés, T.; Dóbé, S. *J. Phys. Chem.* **1998**, 102, 9219.
- (7) Frisch, M. J.; Trucks, G. W.; Schlegel, H. B.; Gill, P. M. W.; Johnson, B. G.; Wong, M. W.; Foresman, J. B.; Robb, M. A.; Head-Gordon, M.; Replogle, E. S.; Gomperts, R.; Andres, J. L.; Raghavachari, K.; Binkley, J. S.; Gonzalez, C.; Martin, R. L.; Fox, D. J.; Defrees, D. J.; Baker, J.; Stewart, J. P.; Pople, J. A., Eds. *Gaussian 92/DFT*, Revision F.2; Gaussian, Inc.: Pittsburgh, PA, 1993. Frisch, M. J.; Trucks, G. W.; Schlegel, H. B.; Gill, P. M. W.; Johnson, B. G.; Robb, M. A.; Cheeseman, J. R.; Keith, T.; Petersson, G. A.; Montgomery, J. A.; Al-Laham, M. A.; Zakrzewski, V. G.; Ortiz, J. V.; Foresman, J. B.; Cioslowski, J.; Stefanov, B. B.; Nanayakkara, A.; Challacombe, M.; Peng, C. Y.; Ayala, P. Y.; Chen, W.; Wong, M. W.; Andres, J. L.; Replogle, E. S.; Gomperts, R.; Martin, R. L.; Fox, D. J.; Binkley, J. S.; Defrees, D. J.; Baker, J.; Stewart, J. P.; Head-Gordon, M.; Gonzalez, C.; Pople, J. A., Eds. *Gaussian 94*, Revision D. 3; Gaussian, Inc.: Pittsburgh, PA, 1995.
- (8) Hehre, W. J.; Radom, L.; Schleyer, P. v. R.; Pople, J. A. *Ab Initio Molecular Orbital Theory*; Wiley: New York, 1986.
- (9) Möller, C.; Plesset, M. S. *Phys. Rev.* **1934**, 46, 618.
- (10) Krishnan, R.; Pople, J. A. *Int. J. Quantum Chem.* **1980**, 14, 91.
- (11) (a) Pople, J. A.; Head-Gordon, M.; Raghavachari, K.; Curtiss, L. A. *J. Chem. Phys.* **1989**, 90, 5622. (b) Curtiss, L. A.; Jones, C.; Trucks, G. W.; Raghavachari, K.; Pople, J. A. *J. Chem. Phys.* **1990**, 93, 2537. (c) Curtiss, L. A.; Raghavachari, K.; Trucks, G. W.; Pople, J. A. *J. Chem. Phys.* **1991**, 94, 7221. (d) Curtiss, L. A.; Raghavachari, K.; Pople, J. A. *J. Chem. Phys.* **1993**, 98, 1293.
- (12) (a) Chase, N. W., Jr.; Davies, C. A.; Downey, J. R., Jr.; Frurip, D. J.; McDonald, R. A.; Syverud, A. N. *J. Phys. Chem. Ref. Data* **1995**, 14 Suppl. 1 (JANAF Thermochemical Tables, 3rd ed.). (b) Glusckko, V. P.; Gurvich, L. V.; Bergman, G. A.; Veyts, I. V.; Medvedev, V. A.; Chachkuruzov, G. A.; Yungman, V. S. *Termodinamicheskoe Svoistva Individualnykh Vestchestv*; Nauka: Moscow, 1974.
- (13) (a) Baker, J. J. *Comput. Chem.* **1986**, 7, 385. (b) Baker, J. J. *Comput. Chem.* **1987**, 8, 563.
- (14) Chen, Y.; Tschuikow-Roux, E. *J. Phys. Chem.* **1993**, 97, 3742.
- (15) DeMore, W. B.; Sander, S. P.; Golden, D. M.; Hampson, R. F.; Kurylo, M. J.; Howard, C. J.; Ravishankara, A. R.; Kolb, C. E.; Molina, M. J. *Chemical Kinetics and Photochemical Data for Use in Stratospheric Modeling*. JPL Publication 94-26; Evaluation No. 11; NASA Panel for Data Evaluation, Jet Propulsion Laboratory, California Institute of Technology: Pasadena, 1994; p 194.
- (16) (a) Troe, J. J. *J. Chem. Phys.* **1981**, 75, 226. (b) Troe, J. J. *J. Chem. Phys.* **1983**, 79, 6017.
- (17) (a) Forst, W.; Prášil, Z. *J. Chem. Phys.* **1969**, 51, 3006. (b) Hoare, M. R. *J. Chem. Phys.* **1970**, 52, 5695.
- (18) Cobos, C. J.; Troe, J. J. *J. Chem. Phys.* **1985**, 83, 1010.
- (19) Chen, Y.; Rauk, A.; Tschuikow-Roux, E. *J. Phys. Chem.* **1991**, 95, 9900.
- (20) Szilágyi, I.; Dóbé, S.; Bércés, T. *Chem. Phys. Lett.* **1998**. To be published.